Additional file 2

Fig. S1. CENH3 ChIP–seq mapping profile of African eggplant (*Solanum aethiopicum*, 'Sa01').

Fig. S2. CENH3 ChIP-seq mapping profile of eggplant (*Solanum melongena*, 'Sm01').

Fig. S3. CENH3 ChIP-seq mapping profile of wild pepper (*Capsicum annuum* var. *glabriusculum* 'Chiltepin 12',).

Fig. S4. CENH3 ChIP-seq mapping profile of pepper (*Capsicum annuum*, 'CA59').

Fig. S5. CENH3 ChIP-seq mapping profile of wild tomato (*Solanum pimpinellifolium*, 'LA1589').

Fig. S6. CENH3 ChIP–seq mapping profile of tomato (*Solanum lycopersicum*, 'Heinz 1706').

Fig. S7. Synteny maps of chromosomes Chr01–Chr06 among wild pepper 'Chiltepin 12', cultivated pepper 'CA59', and the T2T assembly 'G1-36576'.

Fig. S8. Comparison of CENH3-binding profiles between two pepper accessions (top, 'G1-36576'; bottom, 'CA59').

Fig. S9. Comparison of CENH3 ChIP–seq mapping profiles in eggplant (*Solanum melongena*) between two divergent accessions.

Fig. S10. Comparison of CENH3 ChIP–seq mapping profiles in tomato (*Solanum lycopersicum*) between two divergent accessions.

Fig. S11. CENH3 ChIP-seq mapping profile of tobacco (*Nicotiana benthamiana*, LAB strain).

Fig. S12. Genome-wide synteny and CENH3 ChIP–seq mapping profiles between African eggplant (*S. aethiopicum*) and eggplant (*S. melongena*).

Fig. S13. Examples of synteny breakpoint verification using Hi-C contact maps.

Fig. S14. Alignment of synteny blocks from 28 distantly related *Solanum* species relative to tomato (SL5).

Fig. S15. Conservation of syntenic sequence and distribution of synteny breaks along chromosomes inferred from alignments between tomato 'SL5' and three genome sets spanning different divergence levels.

Fig. S16. Enrichment analysis of synteny breaks around CENH3-binding regions.

Fig. S17. Sequence composition of the functional centromeric regions across eight Solanaceae genomes.

Fig. S18. Pairwise sequence similarity between the 6-Mb pericentromeric regions of tomato ('Heinz 1706') and wild tomato *Solanum pimpinellifolium* ('LA1589').

Fig. S19. Distribution of large arrays of 211-bp satellite repeats in the tomato genome.

Fig. S20. Relationship between coding-gene expression and CENH3-binding intensity.

Fig. S21. Pairwise sequence similarity around the functional centromeres of African eggplant.

Fig. S22. Centromere diversity across seven African eggplant accessions.

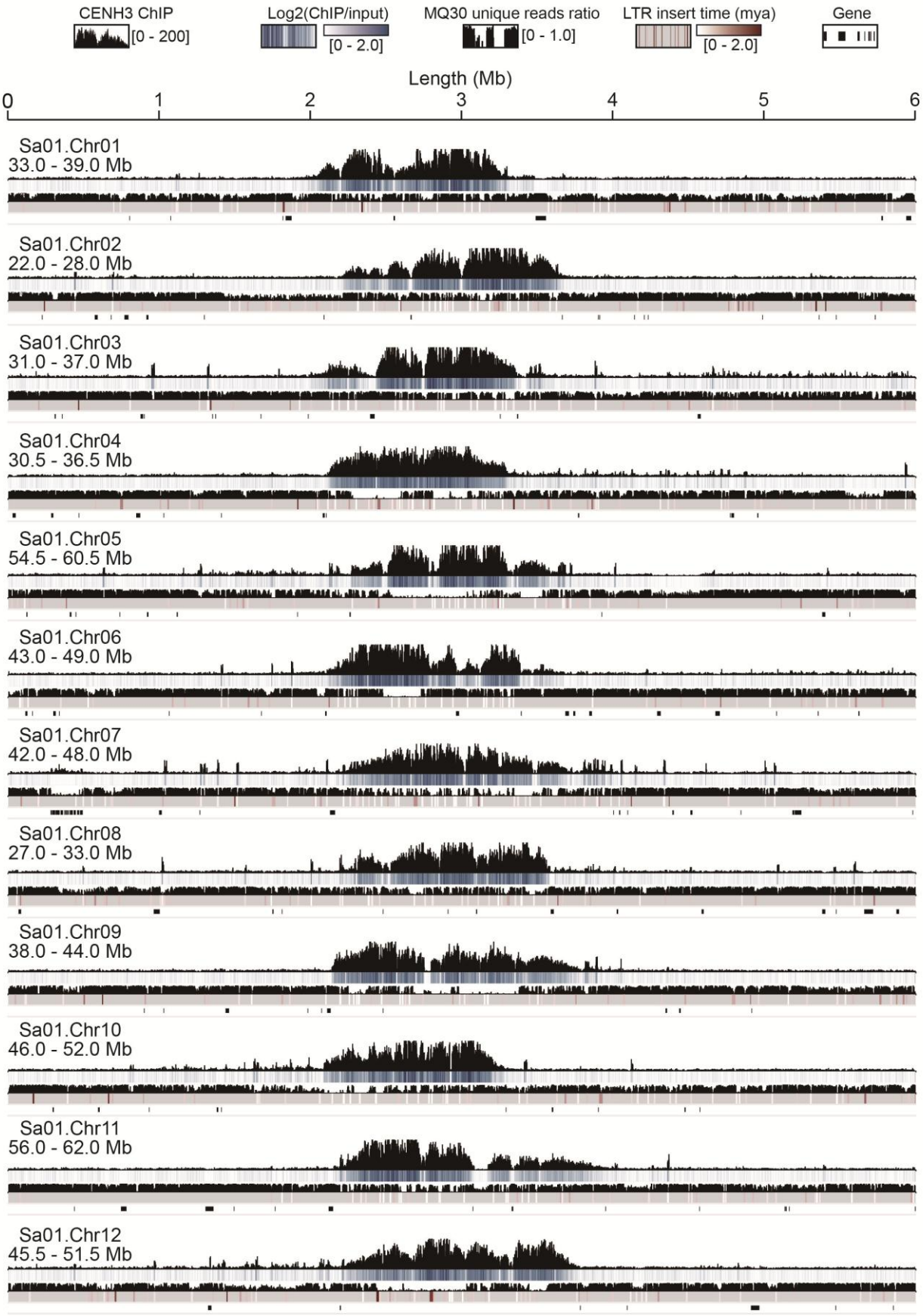

Fig. S1. CENH3 ChIP–seq mapping profile of African eggplant (*Solanum aethiopicum*, 'Sa01'). From top to bottom: CENH3 ChIP–seq peaks, log-transformed ChIP and input signals, unique mapping ratio of MQ30 reads, distribution of intact LTR retrotransposons across centromeric and flanking regions with estimated insertion times, and annotated protein-coding genes.

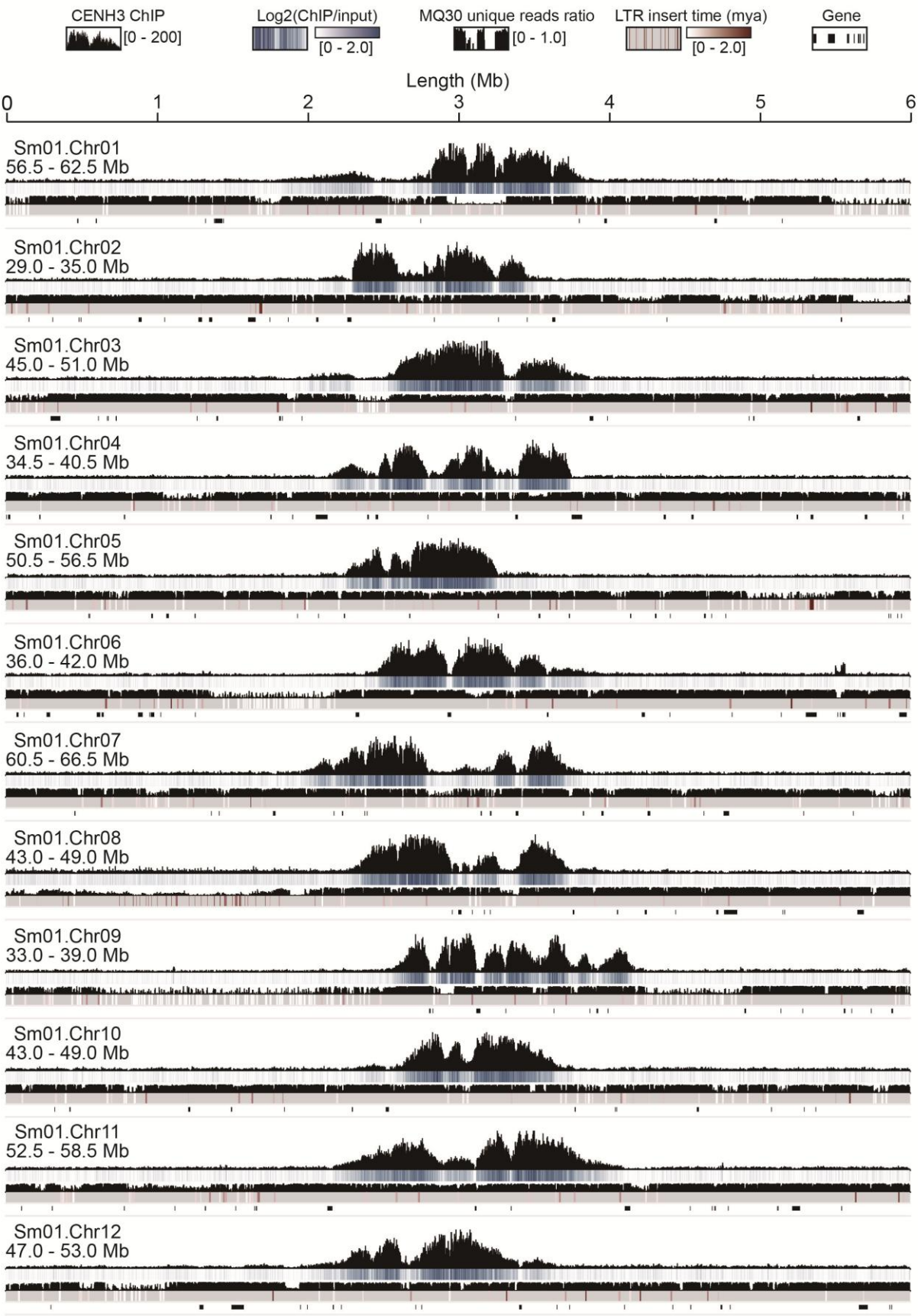

Fig. S2. CENH3 ChIP-seq mapping profile of eggplant (*Solanum melongena*, 'Sm01'). Tracks from top to bottom show CENH3 ChIP–seq peaks, log-transformed ChIP and input signals, unique mapping ratio of MQ30 reads, distribution of intact LTR retrotransposons across centromeric and flanking regions with estimated insertion times, and annotated protein-coding genes.

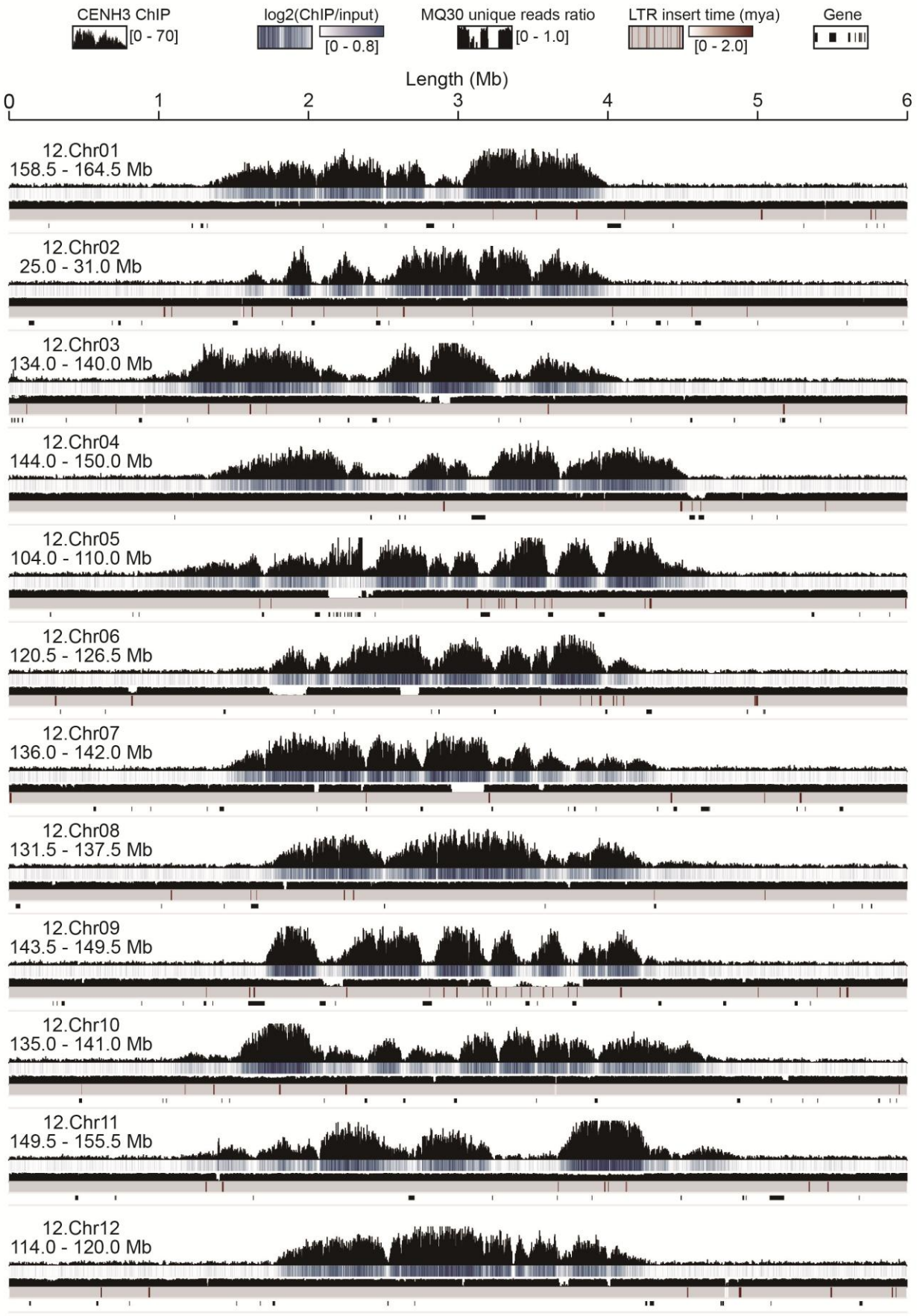

Fig. S3. CENH3 ChIP-seq mapping profile of wild pepper (*Capsicum annuum* var. *glabriusculum* 'Chiltepin 12',). From top to bottom: CENH3 ChIP-seq peaks, log-transformed CENH3 and input signals, unique mapping ratio of MQ30 reads, distribution of intact LTR-retrotransposons across centromeric and surrounding regions with estimated insertion times, and annotated coding genes.

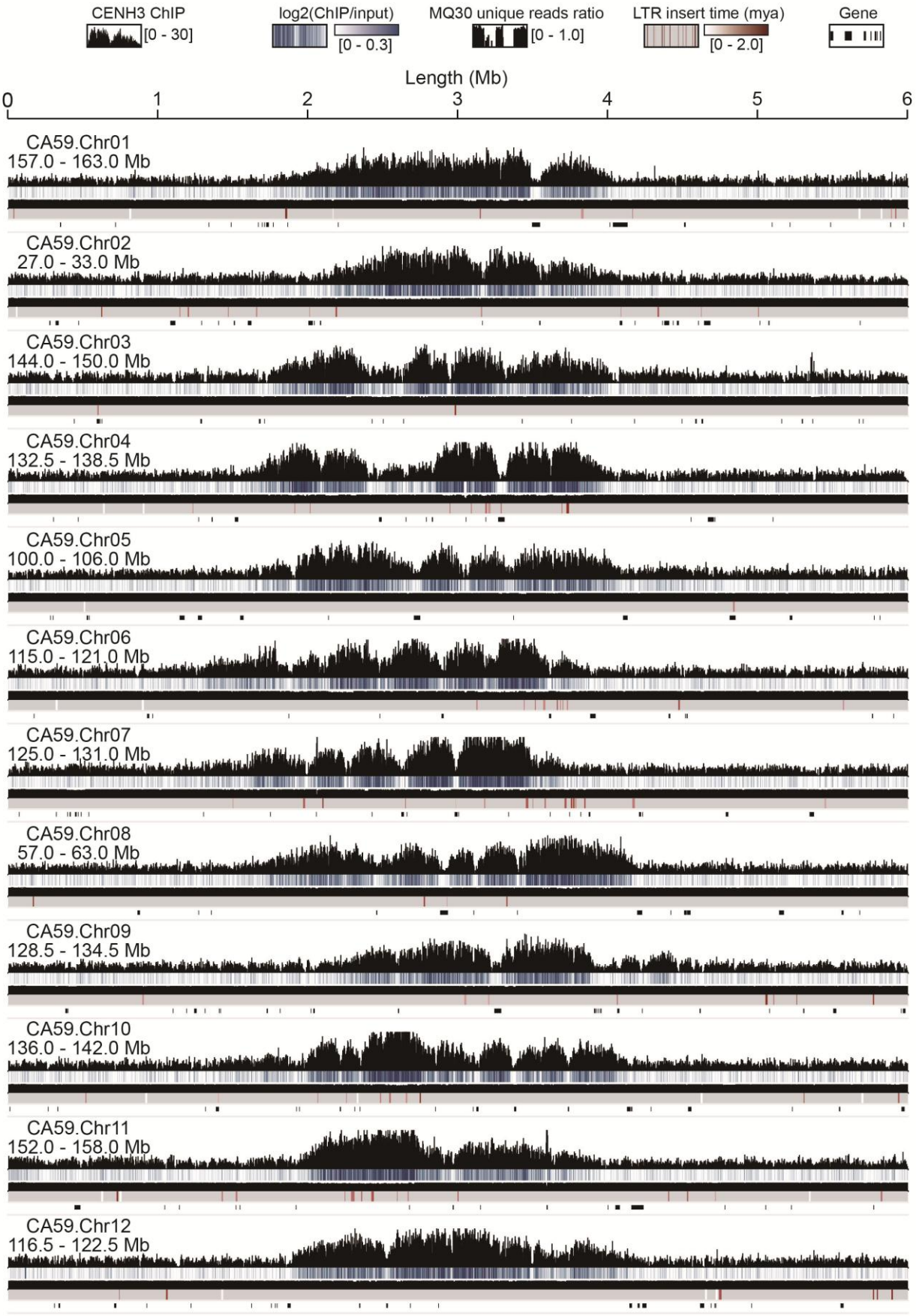

Fig. S4. CENH3 ChIP-seq mapping profile of pepper (*Capsicum annuum*, 'CA59'). From top to bottom: CENH3 ChIP-seq peaks, log-transformed CENH3 and input signals, unique mapping ratio of MQ30 reads, distribution of intact LTR-retrotransposons across centromeric and surrounding regions with estimated insertion times, and annotated coding genes.

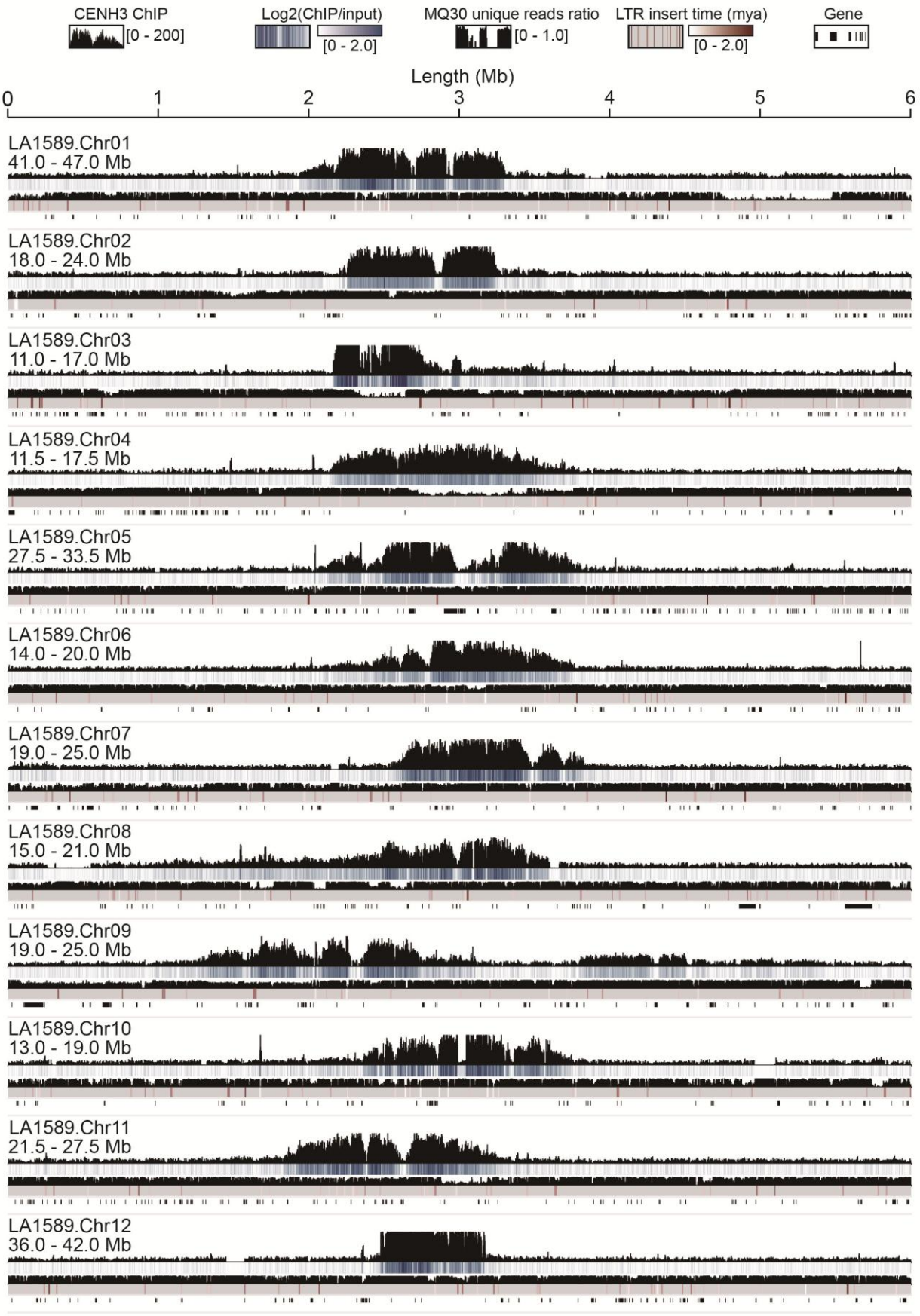

Fig. S5. CENH3 ChIP-seq mapping profile of wild tomato (*Solanum pimpinellifolium*, 'LA1589'). From top to bottom: CENH3 ChIP-seq peaks, log-transformed CENH3 and input signals, unique mapping ratio of MQ30 reads, distribution of intact LTR-retrotransposons across centromeric and surrounding regions with estimated insertion times, and annotated coding genes.

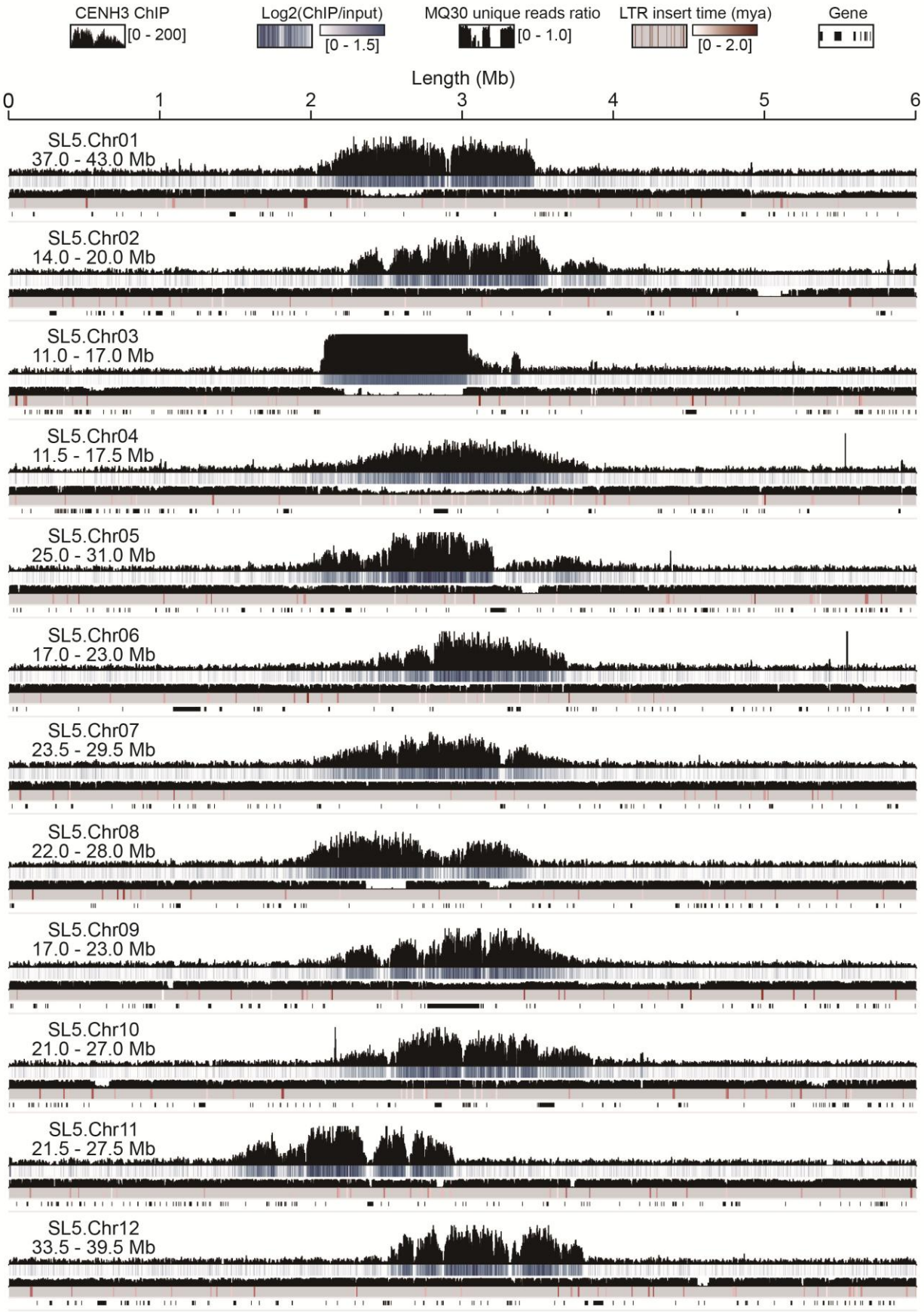

Fig. S6. CENH3 ChIP–seq mapping profile of tomato (*Solanum lycopersicum*, 'Heinz 1706'). From top to bottom: CENH3 ChIP–seq peaks, log-transformed ChIP and input signals, unique mapping ratio of MQ30 reads, distribution of intact LTR retrotransposons across centromeric and flanking regions with estimated insertion times, and annotated protein-coding genes.

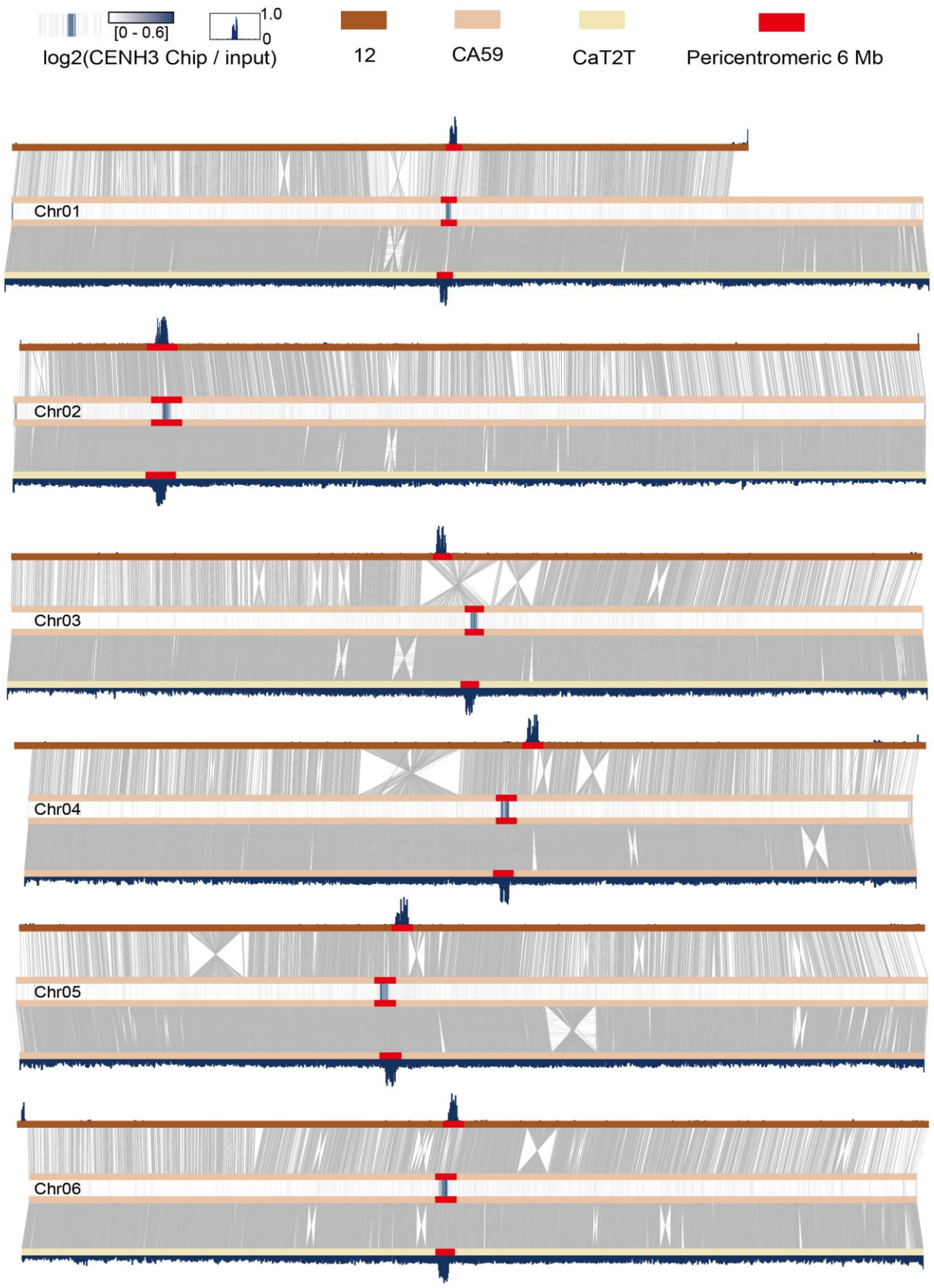

Fig. S7A. Synteny maps of chromosomes Chr01–Chr06 among wild pepper 'Chiltepin 12', cultivated pepper 'CA59', and the T2T assembly 'G1-36576'. Log-transformed CENH3 ChIP–seq/input signals are shown for Chiltepin (top), CA59 (middle), and CaT2T (bottom). Conserved syntenic markers are connected by gray lines.

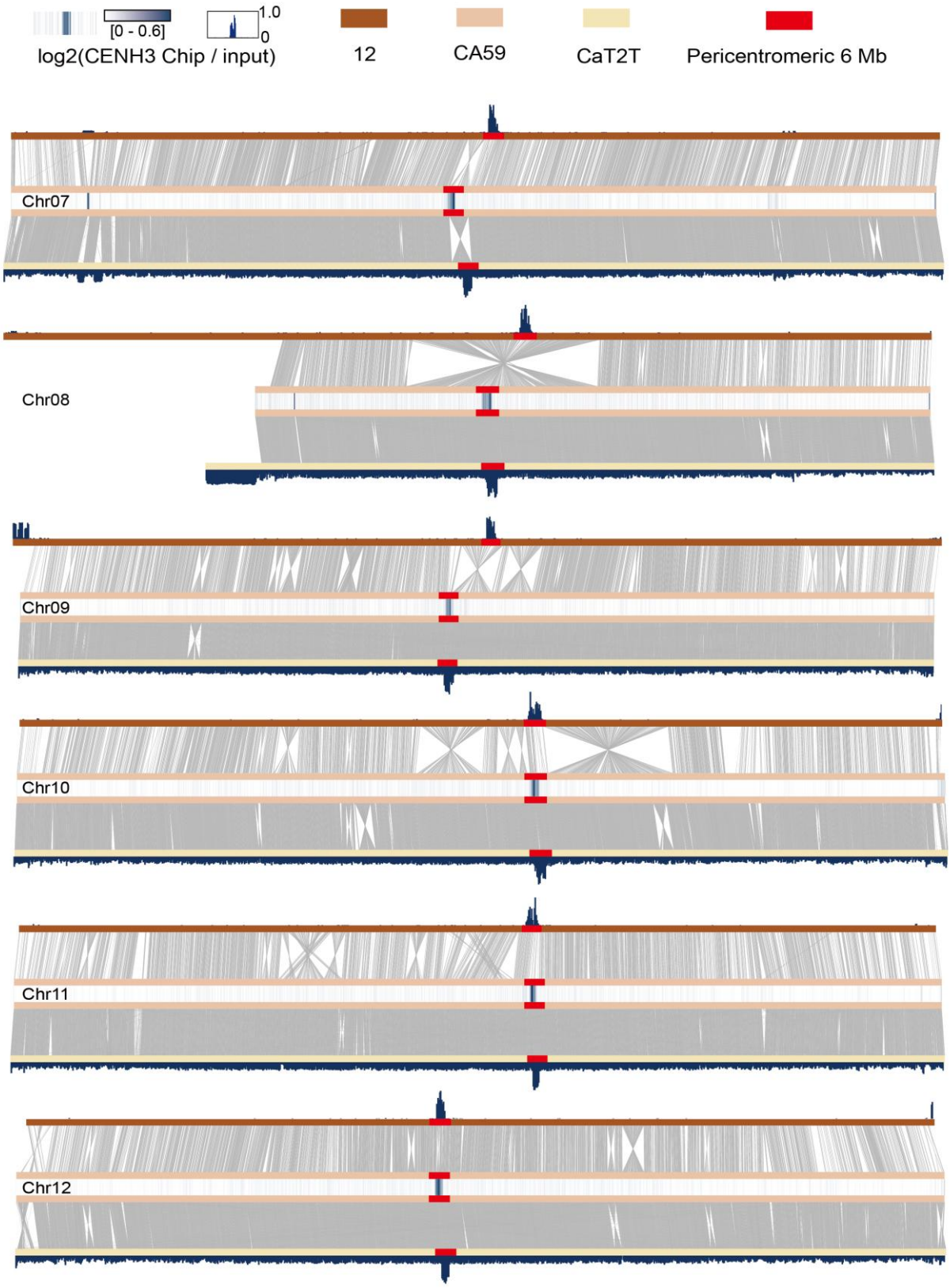

Fig. S7B. Synteny maps of chromosomes Chr08–Chr12 among wild pepper 'Chiltepin 12', cultivated pepper 'CA59', and the T2T assembly 'G1-36576'. Log-transformed CENH3 ChIP–seq/input signals are shown for Chiltepin (top), CA59 (middle), and CaT2T (bottom). Conserved syntenic markers are connected by gray lines.

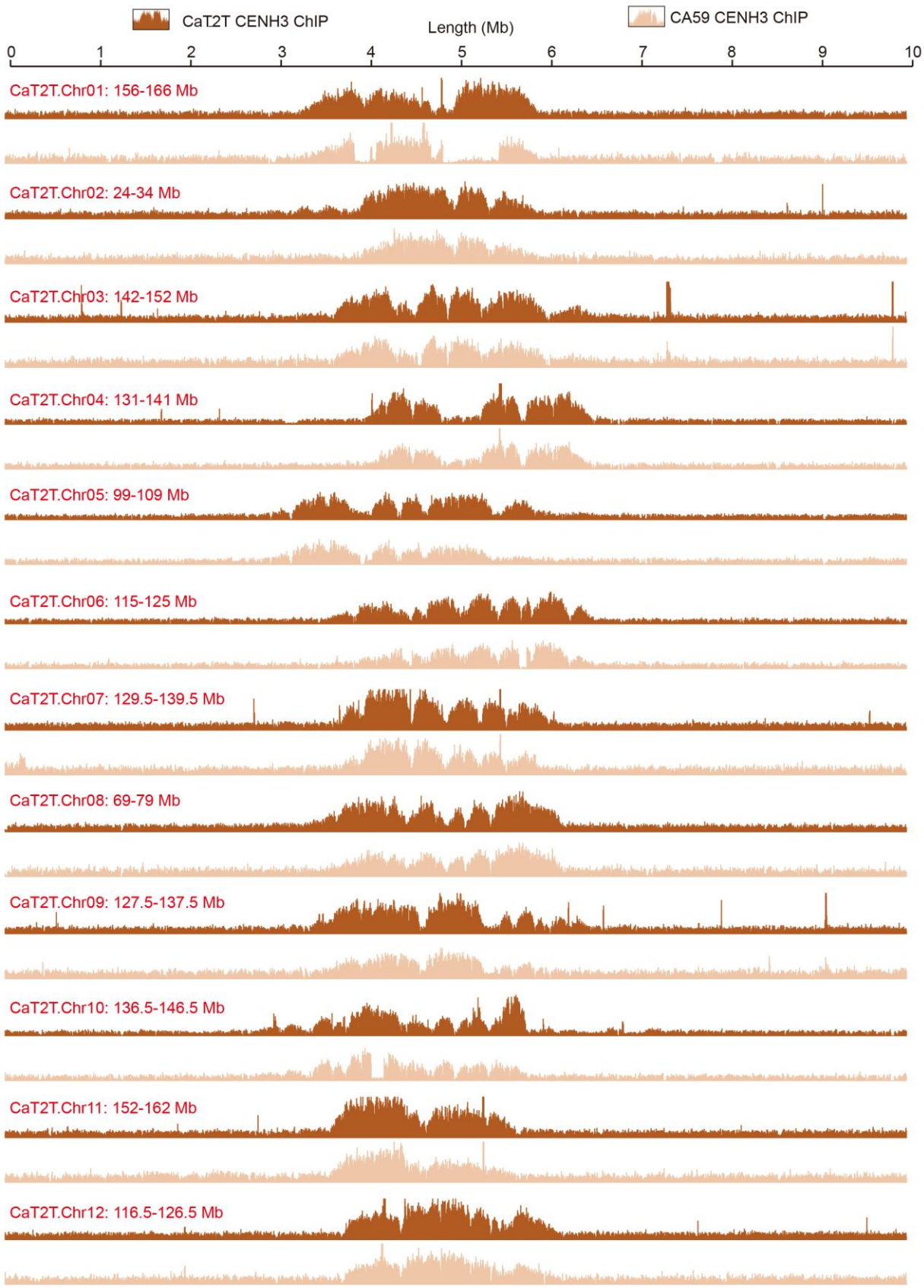

Fig. S8. Comparison of CENH3-binding profiles between two pepper accessions (top, 'G1-36576'; bottom, 'CA59'). CENH3 ChIP–seq reads from both accessions were aligned to the 'G1-36576' reference genome to enable direct comparison of enrichment patterns.

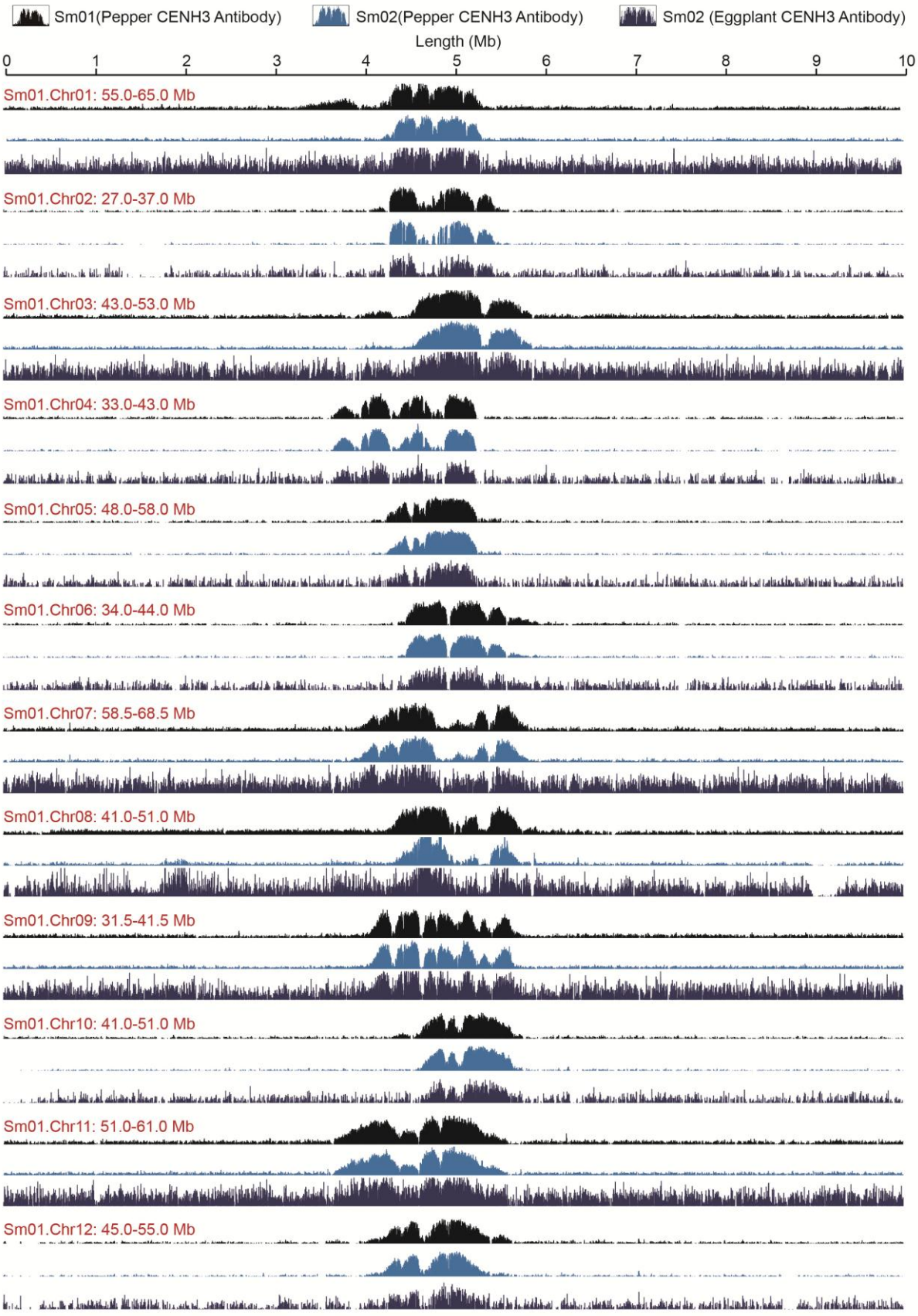

Fig. S9. Comparison of CENH3 ChIP–seq mapping profiles in eggplant (*Solanum melongena*) between two divergent accessions. CENH3 ChIP–seq was performed for 'Sm01' and 'Sm02', and reads from both accessions were aligned to the 'Sm01' reference genome. Peaks show enrichment as $\log_2$(CENH3 ChIP/Input). For 'Sm02', two biological replicates were also generated using pepper- and eggplant-derived anti-CENH3 antibodies.

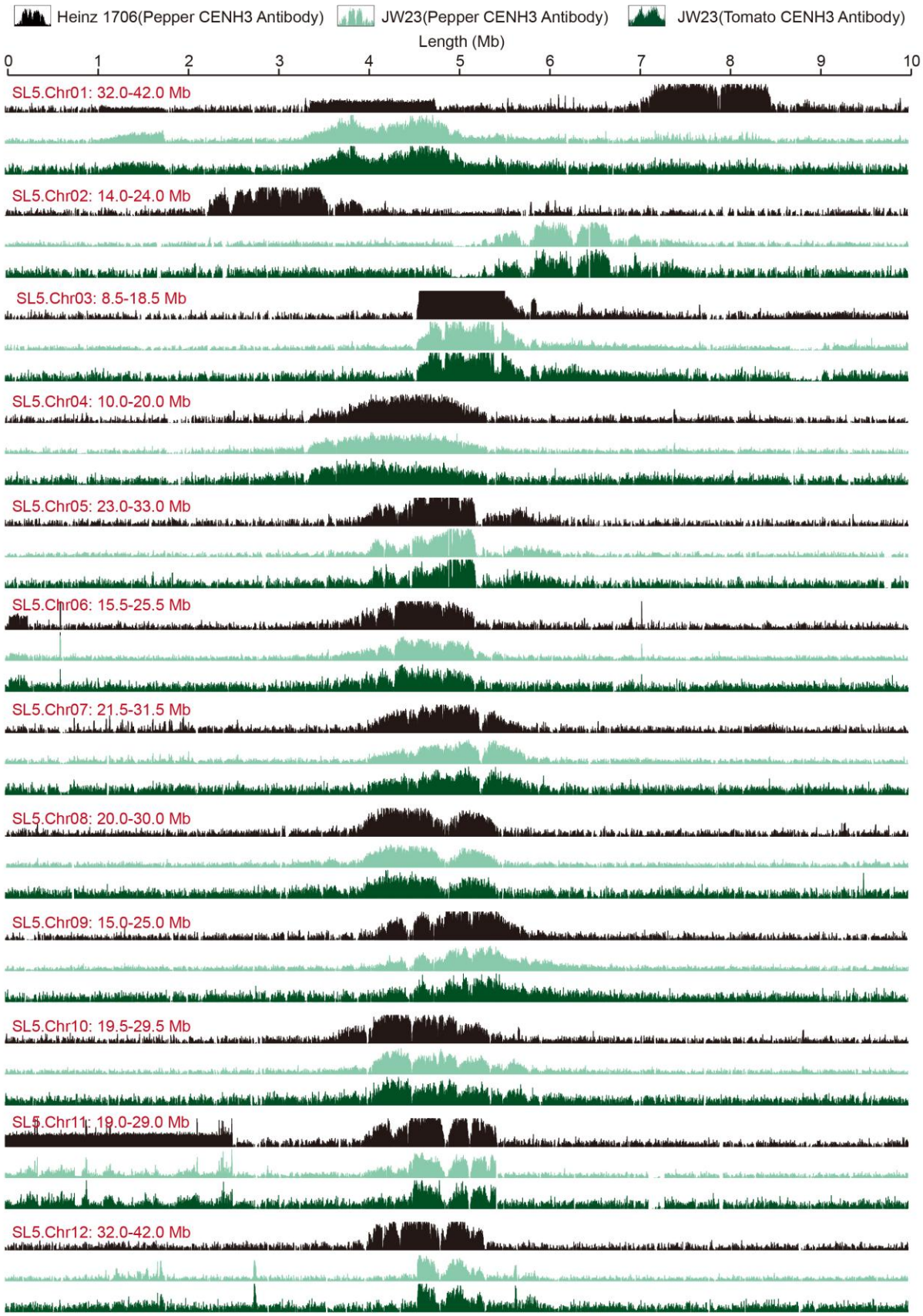

Fig. S10. Comparison of CENH3 ChIP–seq mapping profiles in tomato (*Solanum lycopersicum*) between two divergent accessions. CENH3 ChIP–seq was performed for 'Heinz 1706' and 'JW23', and reads from both accessions were aligned to the SL5 reference genome. Peaks show enrichment as $\log_2$(CENH3 ChIP/Input). For 'JW23', two biological replicates were also generated using pepper- and eggplant-derived anti-CENH3 antibodies.

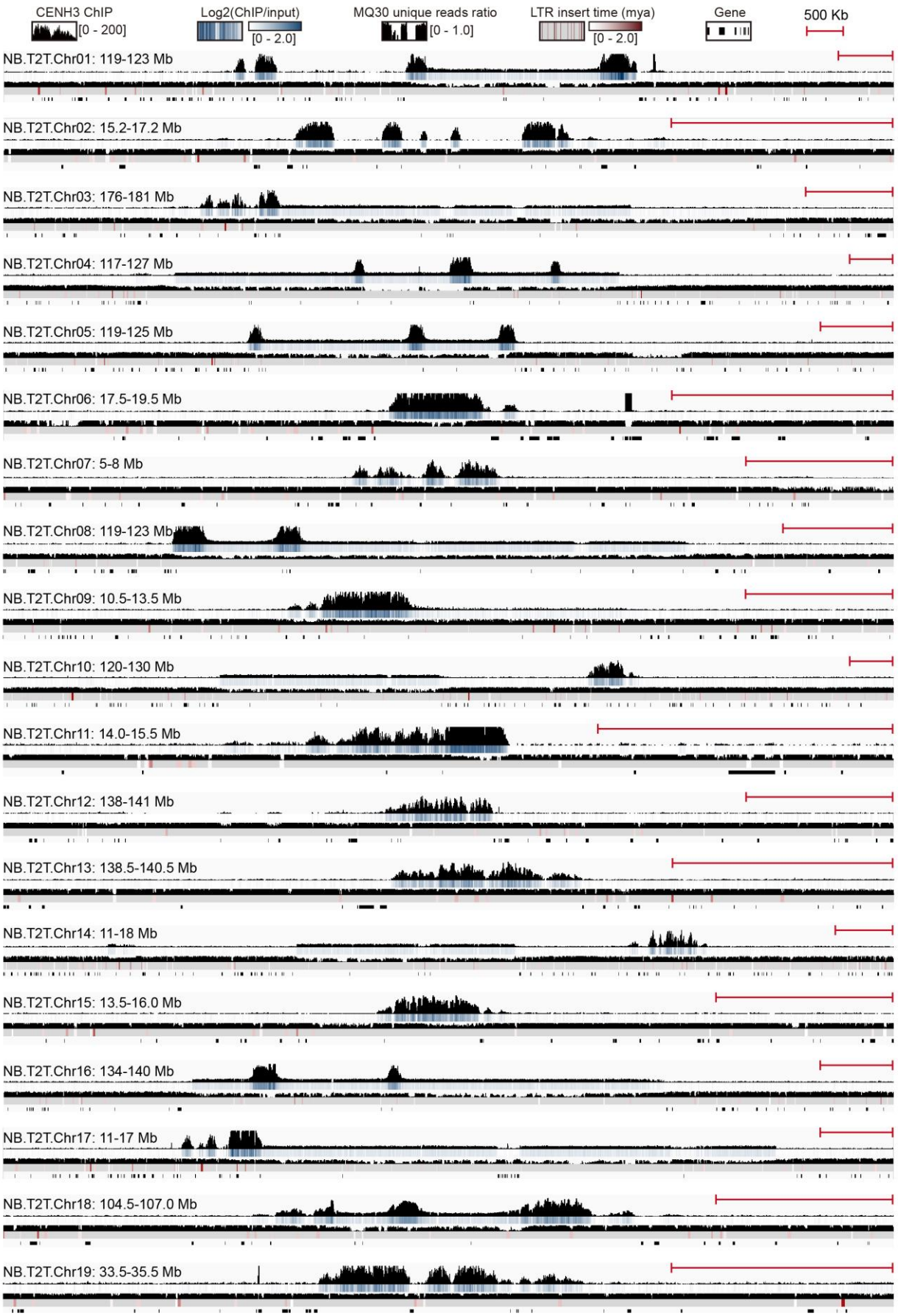

Fig. S11. CENH3 ChIP-seq mapping profile of tobacco (*Nicotiana benthamiana*, LAB strain). Public CENH3 ChIP-seq reads were aligned to the NB.T2T reference genome, and peaks were identified using the same method applied to our newly investigated Solanaceae genomes.

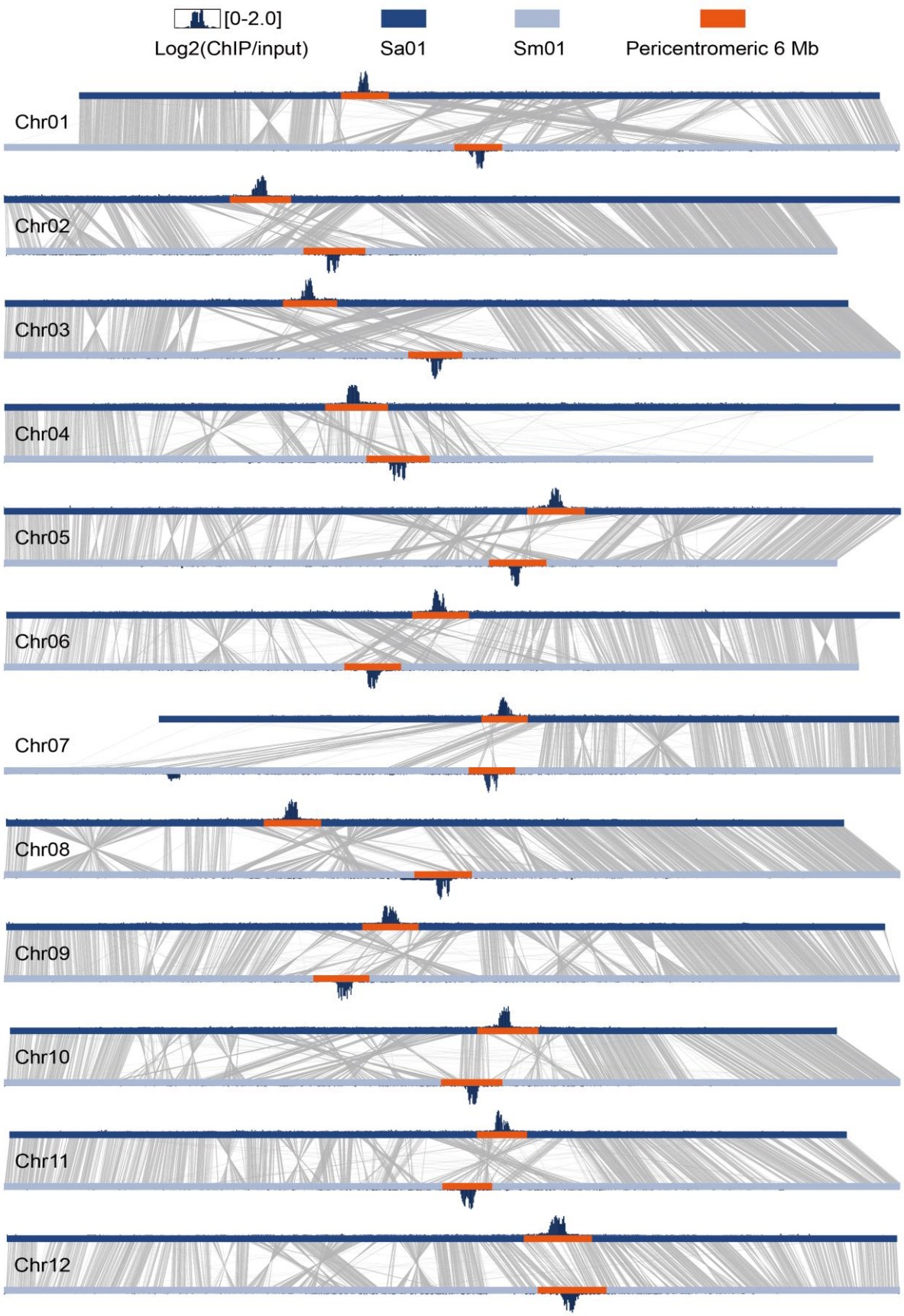

Fig. S12. Genome-wide synteny and CENH3 ChIP–seq mapping profiles between African eggplant (*S. aethiopicum*) and eggplant (*S. melongena*). Log-transformed CENH3 ChIP/Input signals are shown for African eggplant (top) and eggplant (bottom). Conserved syntenic markers are indicated by gray lines, and the 6-Mb regions surrounding CENH3-enriched chromatin are highlighted in orange.

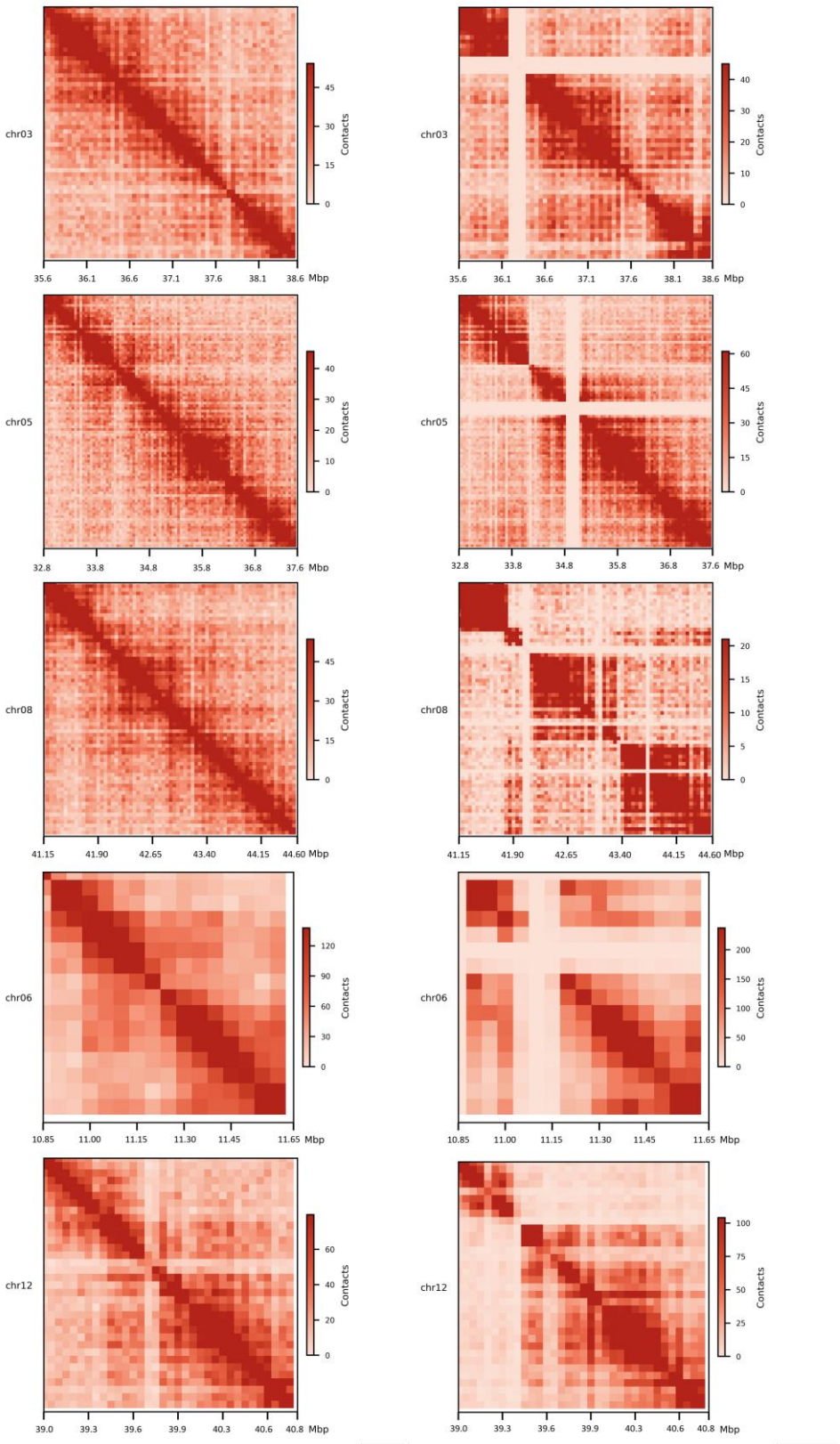

Fig. S13. Examples of synteny breakpoint verification using Hi-C contact maps. Hi-C data from the cultivated tomato accession 'M82' and two wild tomato species, *Solanum pimpinellifolium* (ZY57) and *Solanum galapagense* (ZY56), were aligned to the reference genome SL5. For each synteny breakpoint, Hi-C contact maps were extracted for the corresponding regions (≥500 kb on each side). The left panels show Hi-C maps for 'M82', which recapitulate the SL5 reference configuration. The right panels show the corresponding regions for ZY57 (top 3 maps) and ZY56 (bottom 2 maps), where altered contact patterns support the inferred synteny breakpoints.

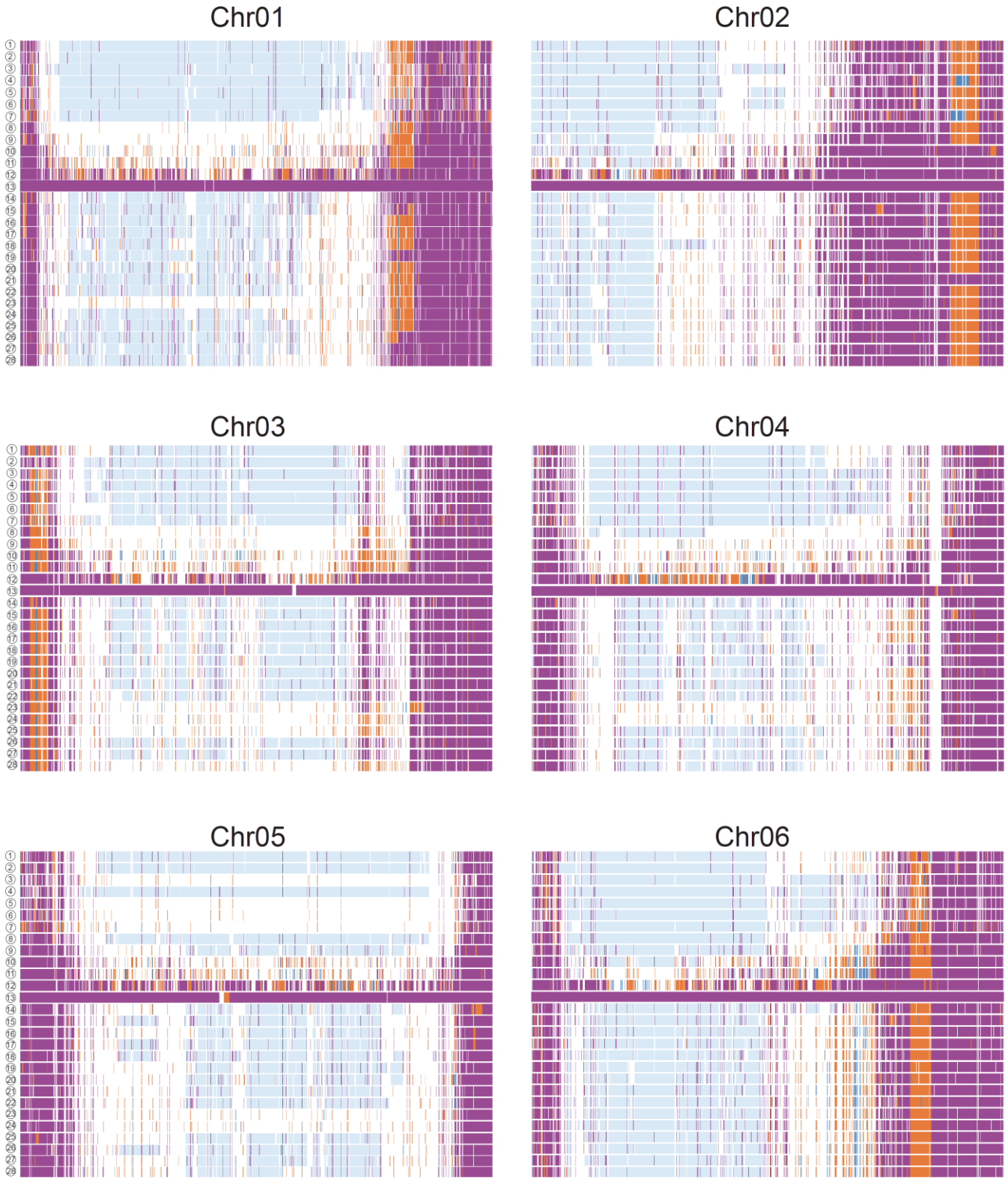

Fig. S14A. Alignment of synteny blocks from 28 distantly related *Solanum* species relative to tomato (SL5). Purple, orange, and blue rectangles denote syntenic blocks, whereas gray rectangles indicate non-syntenic regions and white rectangles represent sequence gaps. Chromosomes 1–6 are shown.

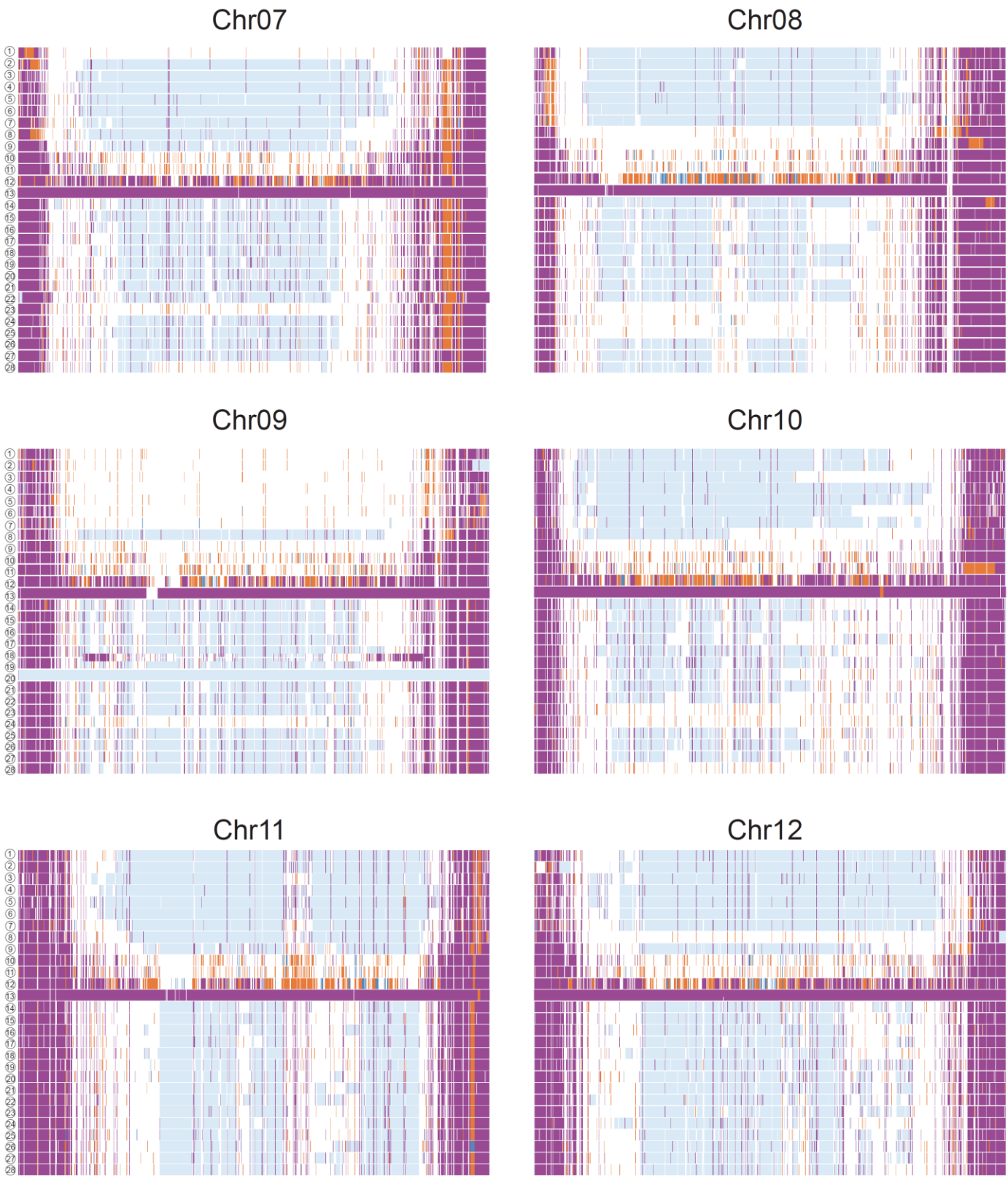

Fig. S14B. Alignment of synteny blocks from 28 distantly related *Solanum* species relative to tomato (SL5). Purple, orange, and blue rectangles denote syntenic blocks, whereas gray rectangles indicate non-syntenic regions and white rectangles represent sequence gaps. Chromosomes 7–12 are shown.

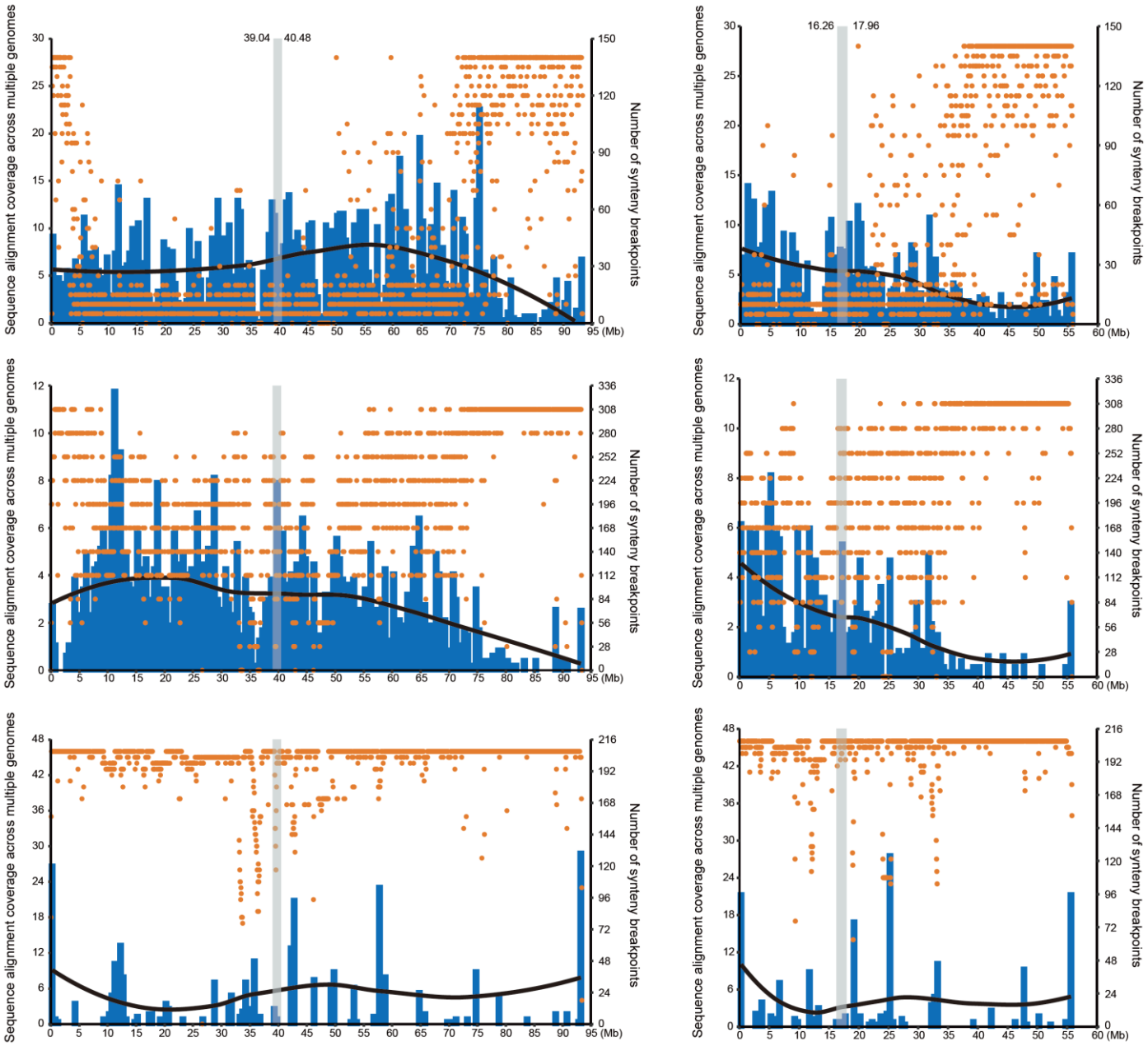

Fig. S15A. Conservation of syntenic sequence and distribution of synteny breaks along chromosomes inferred from alignments between tomato 'SL5' and three genome sets spanning different divergence levels. From top to bottom: 28 distantly related *Solanum* species, 11 closely related species, and 48 tomato accessions. Orange dots indicate, for each genomic window, the number of genomes that align to the reference (left y-axis), and blue bars show the number of synteny breaks in 500-kb windows (right y-axis). Functional centromeric regions are highlighted in gray. Chromosome 1 (left) and chromosome 2 (right) are shown.

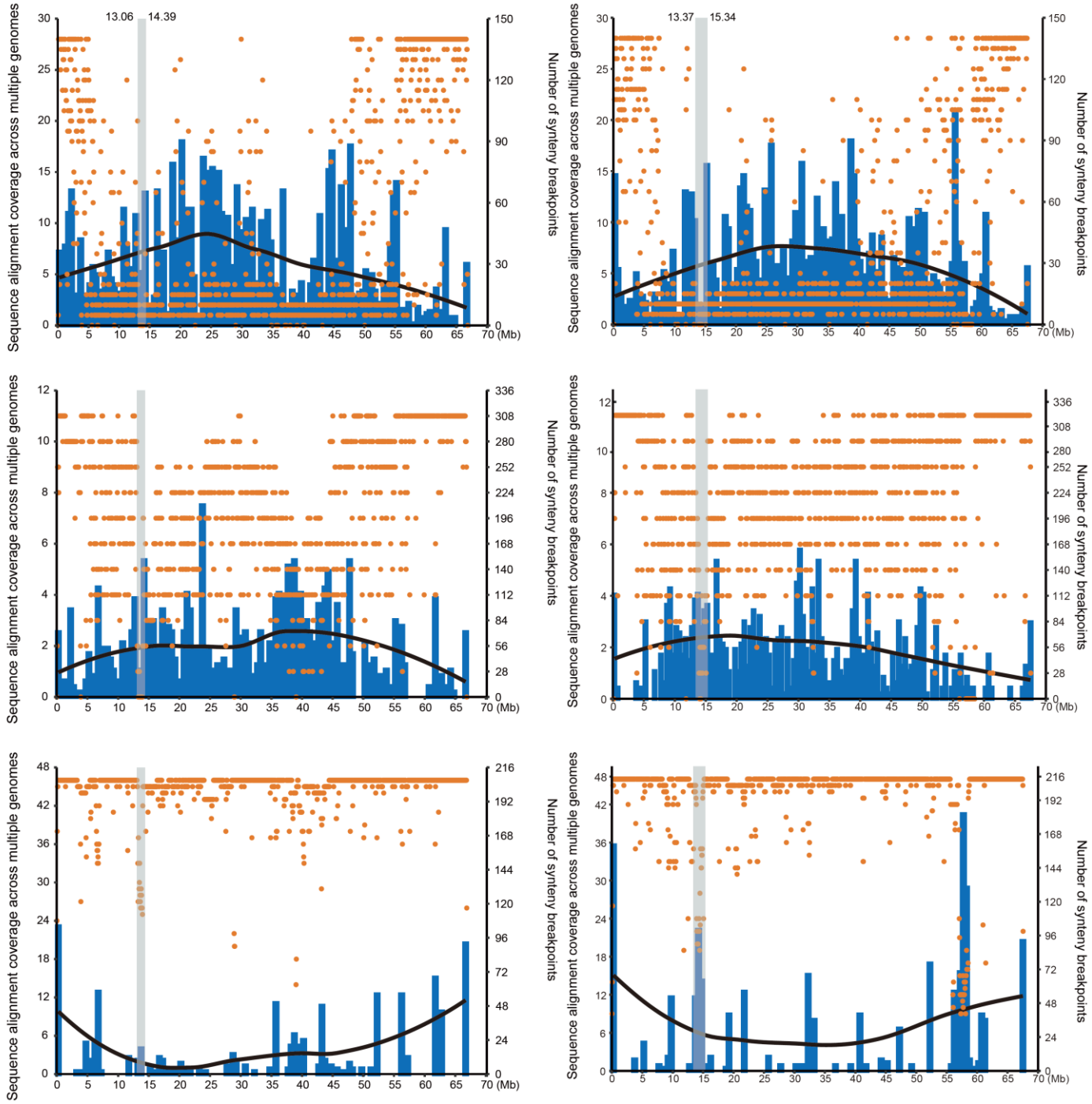

Fig. S15B. Conservation of syntenic sequence and distribution of synteny breaks along chromosomes inferred from alignments between tomato 'SL5' and three genome sets spanning different divergence levels. From top to bottom: 28 distantly related *Solanum* species, 11 closely related species, and 48 tomato accessions. Orange dots indicate, for each genomic window, the number of genomes that align to the reference (left y-axis), and blue bars show the number of synteny breaks in 500-kb windows (right y-axis). Functional centromeric regions are highlighted in gray. Chromosome 3 (left) and chromosome 4 (right) are shown.

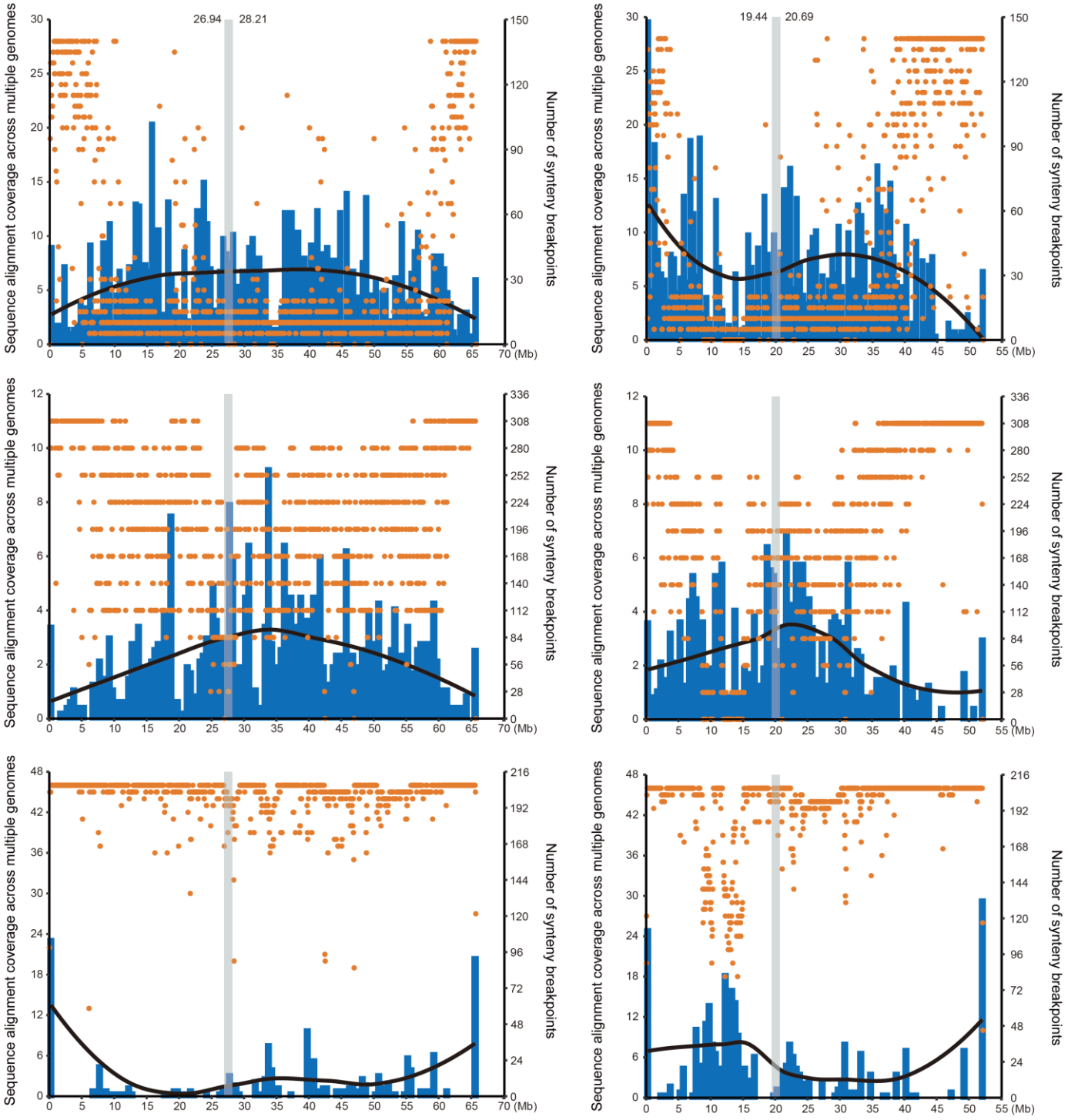

Fig. S15C. Conservation of syntenic sequence and distribution of synteny breaks along chromosomes inferred from alignments between tomato 'SL5' and three genome sets spanning different divergence levels. From top to bottom: 28 distantly related *Solanum* species, 11 closely related species, and 48 tomato accessions. Orange dots indicate, for each genomic window, the number of genomes that align to the reference (left y-axis), and blue bars show the number of synteny breaks in 500-kb windows (right y-axis). Functional centromeric regions are highlighted in gray. Chromosome 5 (left) and chromosome 6 (right) are shown.

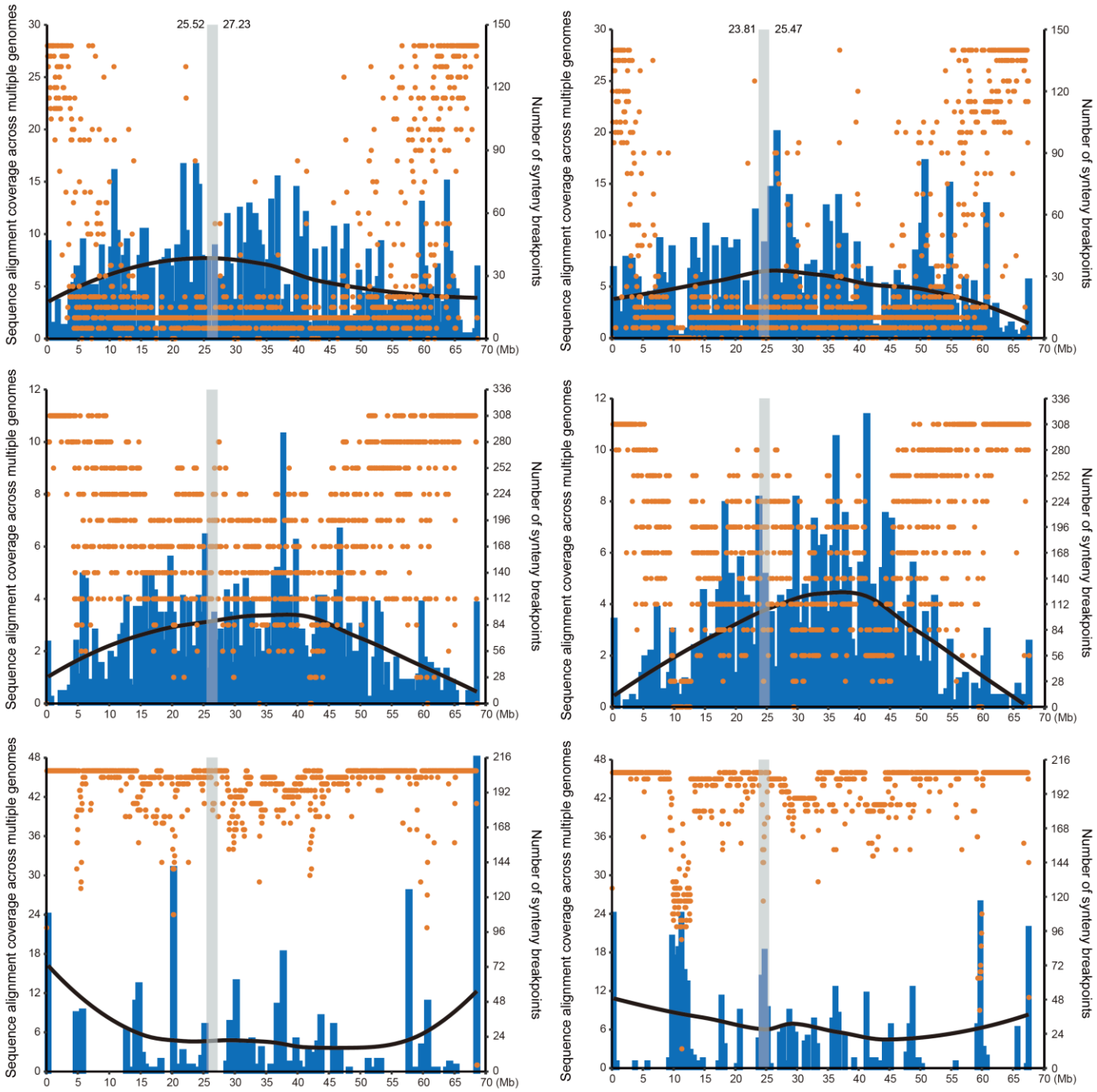

Fig. S15D. Conservation of syntenic sequence and distribution of synteny breaks along chromosomes inferred from alignments between tomato 'SL5' and three genome sets spanning different divergence levels. From top to bottom: 28 distantly related *Solanum* species, 11 closely related species, and 48 tomato accessions. Orange dots indicate, for each genomic window, the number of genomes that align to the reference (left y-axis), and blue bars show the number of synteny breaks in 500-kb windows (right y-axis). Functional centromeric regions are highlighted in gray. Chromosome 7 (left) and chromosome 8 (right) are shown.

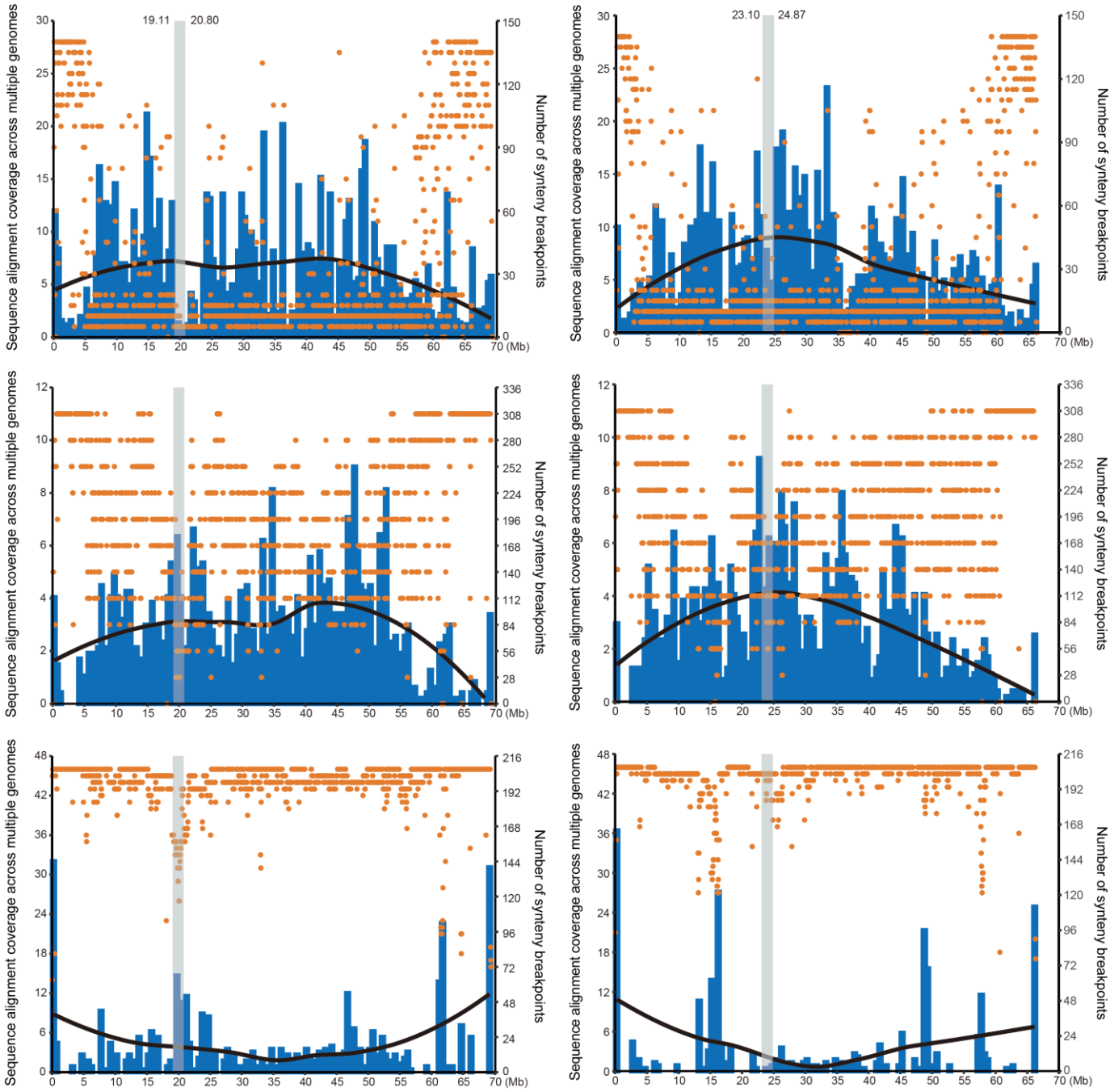

Fig. S15E. Conservation of syntenic sequence and distribution of synteny breaks along chromosomes inferred from alignments between tomato 'SL5' and three genome sets spanning different divergence levels. From top to bottom: 28 distantly related *Solanum* species, 11 closely related species, and 48 tomato accessions. Orange dots indicate, for each genomic window, the number of genomes that align to the reference (left y-axis), and blue bars show the number of synteny breaks in 500-kb windows (right y-axis). Functional centromeric regions are highlighted in gray. Chromosome 9 (left) and chromosome 10 (right) are shown.

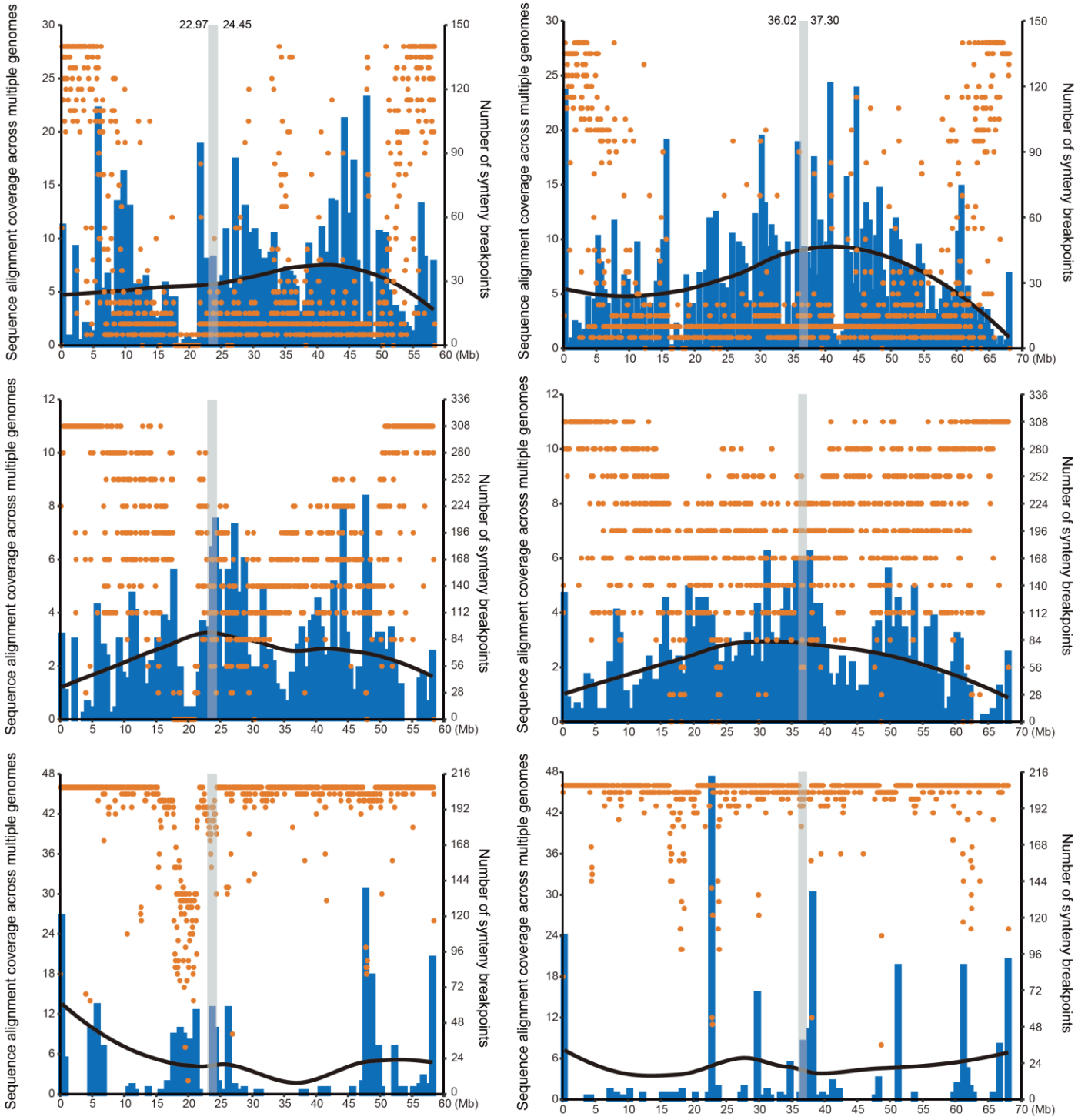

Fig. S15F. Conservation of syntenic sequence and distribution of synteny breaks along chromosomes inferred from alignments between tomato 'SL5' and three genome sets spanning different divergence levels. From top to bottom: 28 distantly related *Solanum* species, 11 closely related species, and 48 tomato accessions. Orange dots indicate, for each genomic window, the number of genomes that align to the reference (left y-axis), and blue bars show the number of synteny breaks in 500-kb windows (right y-axis). Functional centromeric regions are highlighted in gray. Chromosome 11 (left) and chromosome 12 (right) are shown.

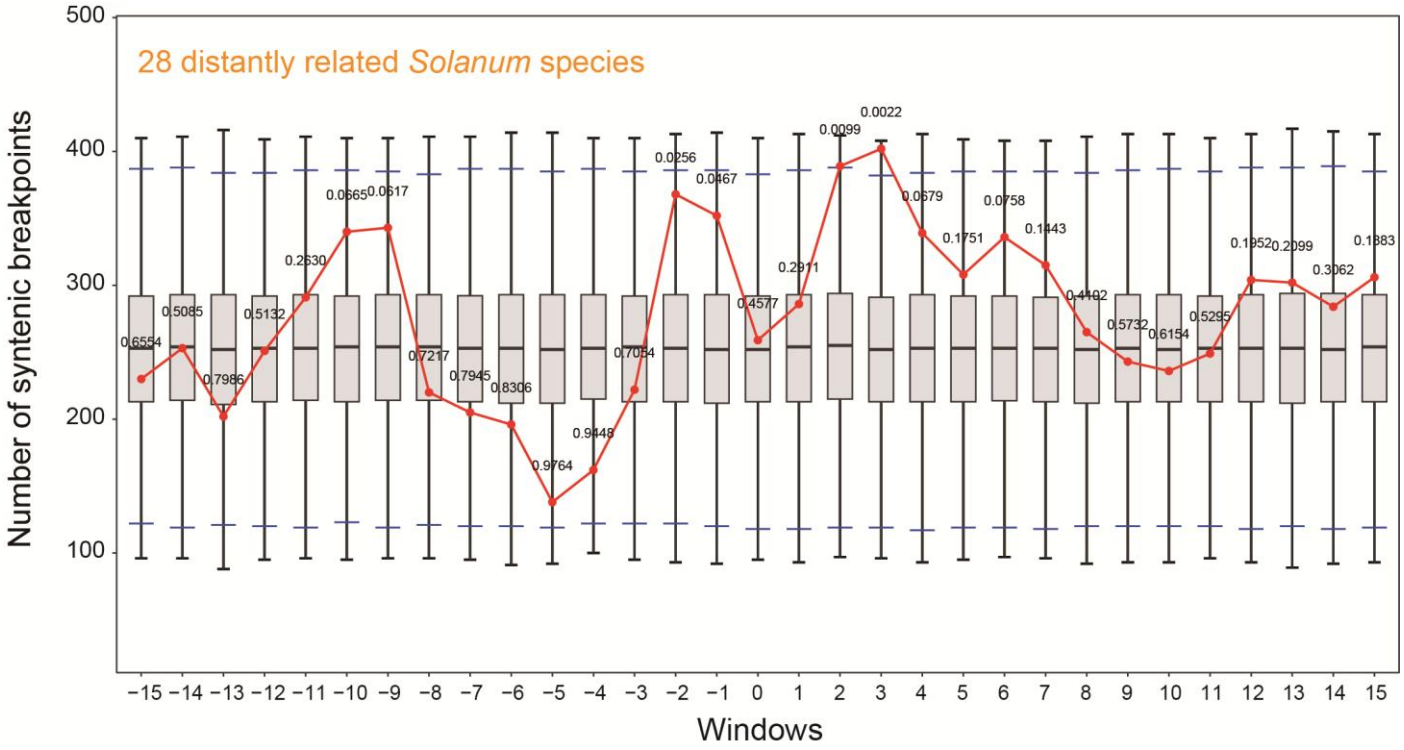

Fig. S16. Enrichment analysis of synteny breaks around CENH3-binding regions. Windows extend on both sides of each functional centromere; for each chromosome, window size was set to the centromere length and slid in steps of half the centromere length. For each window, expected break counts were estimated by permutation (10,000 simulations). Observed values are shown as red dots, and 99% confidence intervals are indicated by blue lines; permutation *P*-values are reported for each window. Synteny breaks were identified using 28 distantly related *Solanum* species.

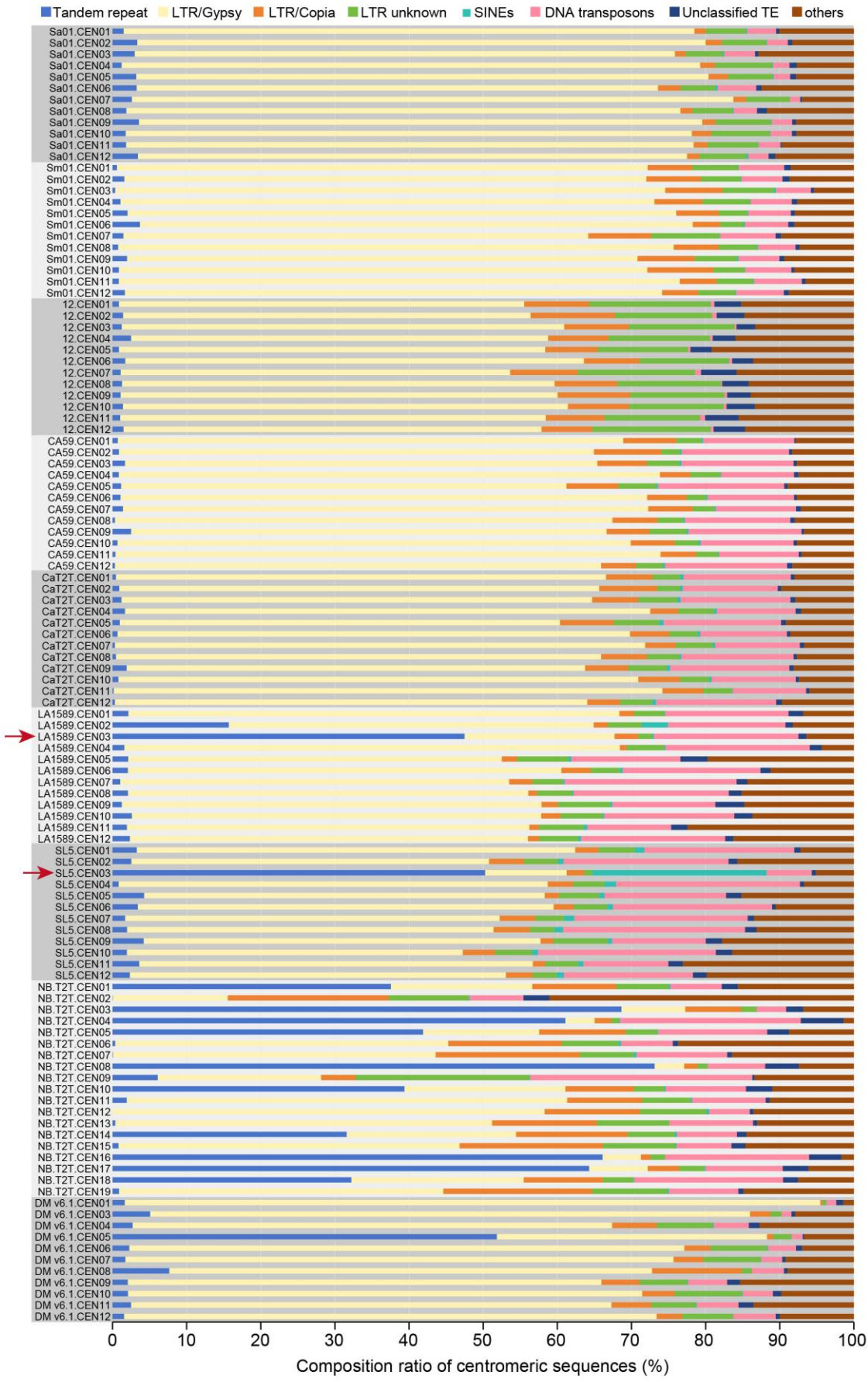

Fig. S17. Sequence composition of the functional centromeric regions across eight Solanaceae genomes. Red arrows highlight the substantially higher proportion of tandem repeats in CEN03 of tomato and wild tomato compared to other centromeric sequences.

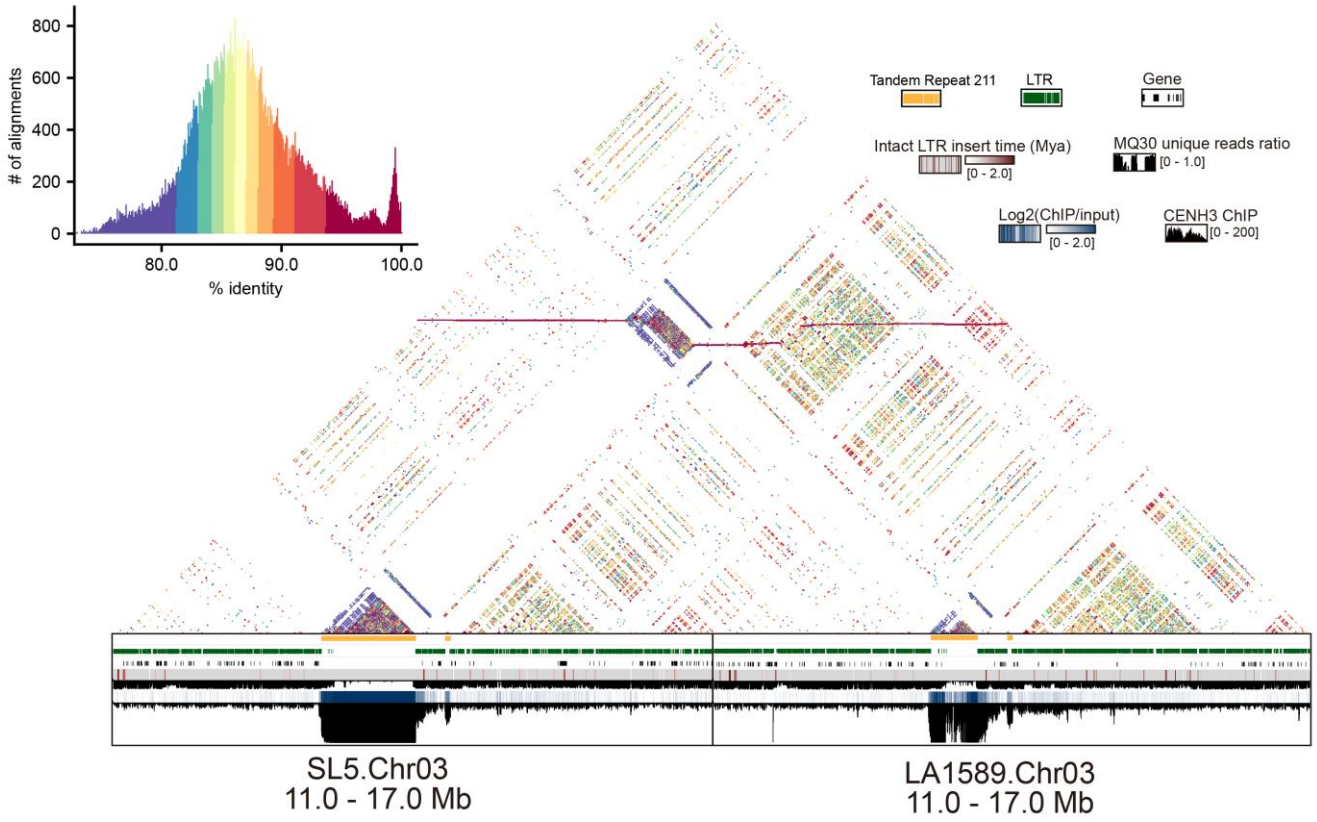

Fig. S18. Pairwise sequence similarity between the 6-Mb pericentromeric regions of tomato ('Heinz 1706') and wild tomato *Solanum pimpinellifolium* ('LA1589').

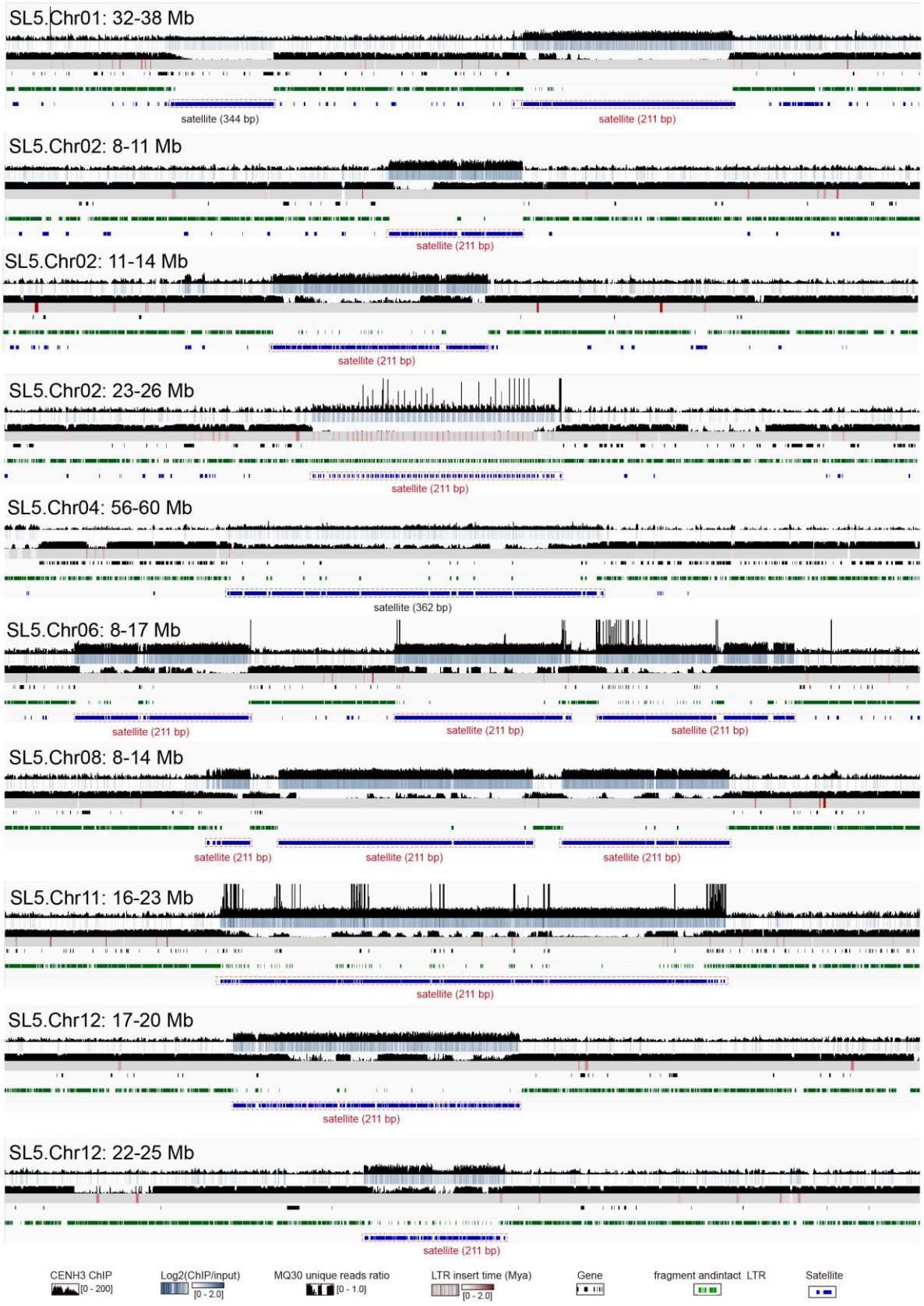

Fig. S19. Distribution of large arrays of 211-bp satellite repeats in the tomato genome. From top to bottom: CENH3 ChIP–seq peaks; log-transformed CENH3 and input signals; unique mapping ratio of MQ30 reads; distribution of intact LTR retrotransposons across centromeric and flanking regions with estimated insertion times; annotated coding genes; fragmented and intact LTRs; and satellite repeats. Arrays of the 211-bp satellite are highlighted with red dashed rectangles.

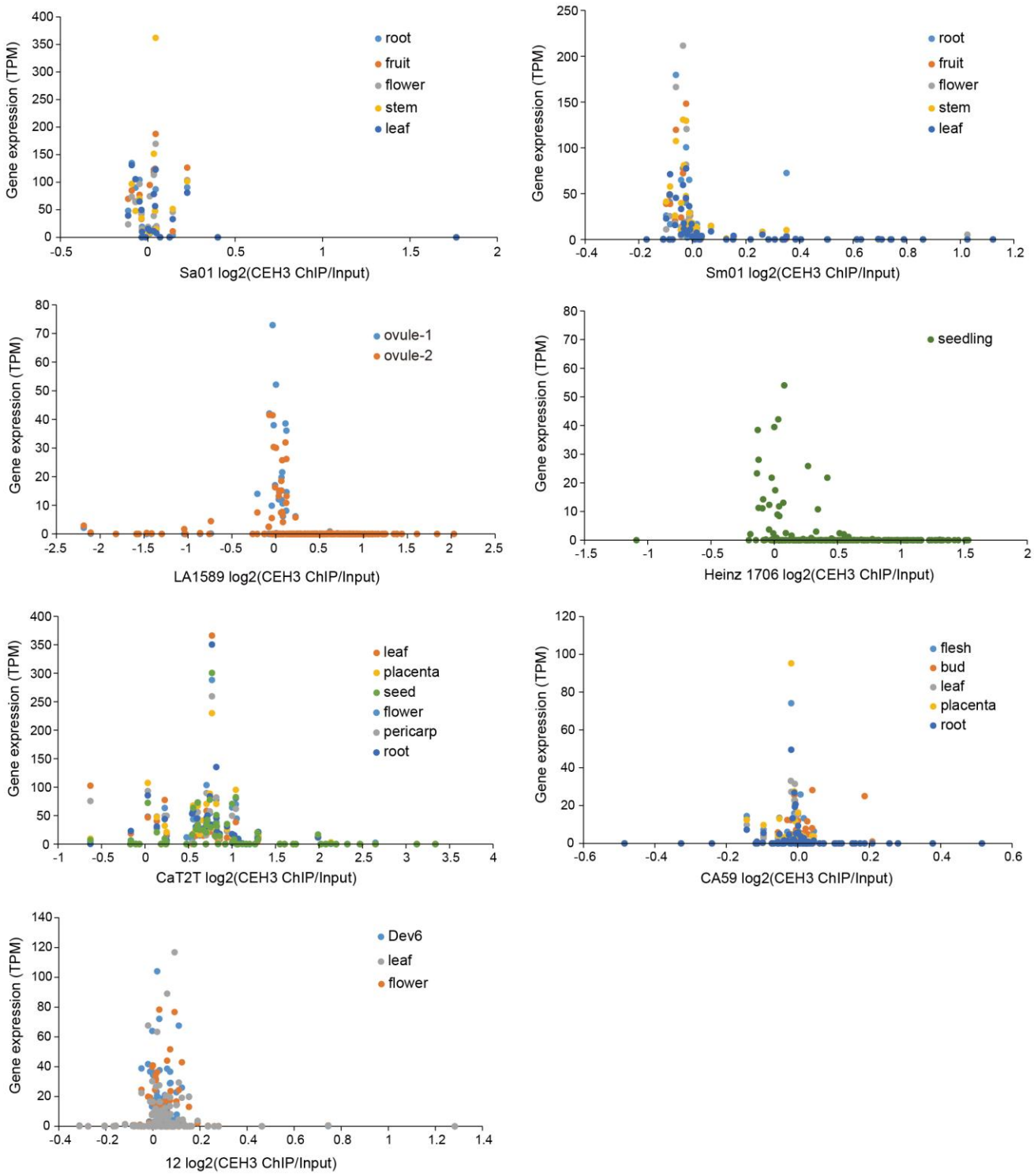

Fig. S20. Relationship between coding-gene expression and CENH3-binding intensity. The x-axis shows the log-transformed CENH3 ChIP–seq signal (ChIP/Input), and the y-axis shows gene expression in TPM (transcripts per million). Each dot represents a gene, with colors indicating different tissues or RNA samples.

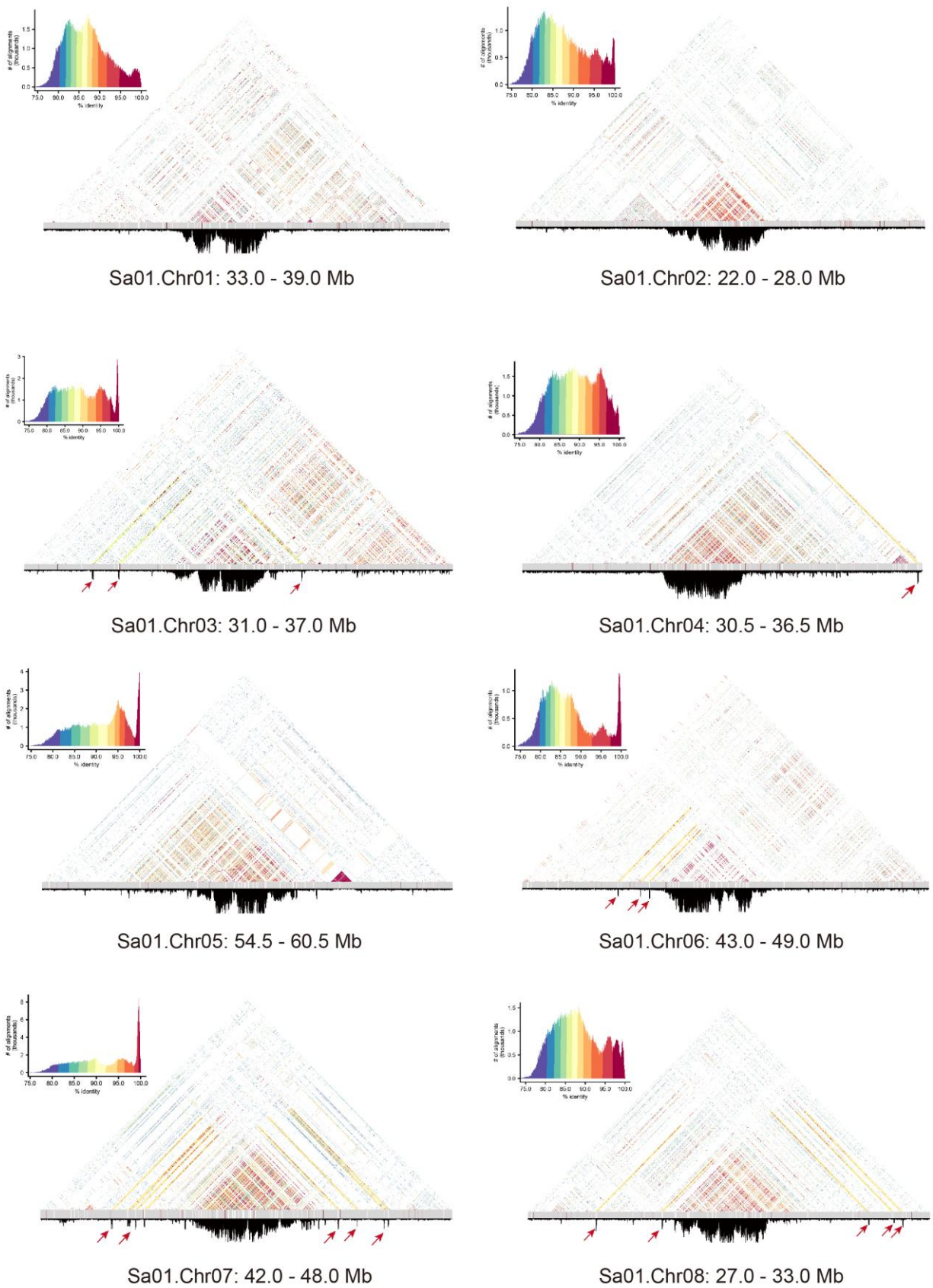

Fig. S21A. Pairwise sequence similarity around the functional centromeres of African eggplant. Heatmaps show the percentage sequence identity in pairwise 100-bp windows. Red arrows indicate potential artificial CENH3-binding peaks outside the functional centromeric regions. Chromosomes 1–8 are shown.

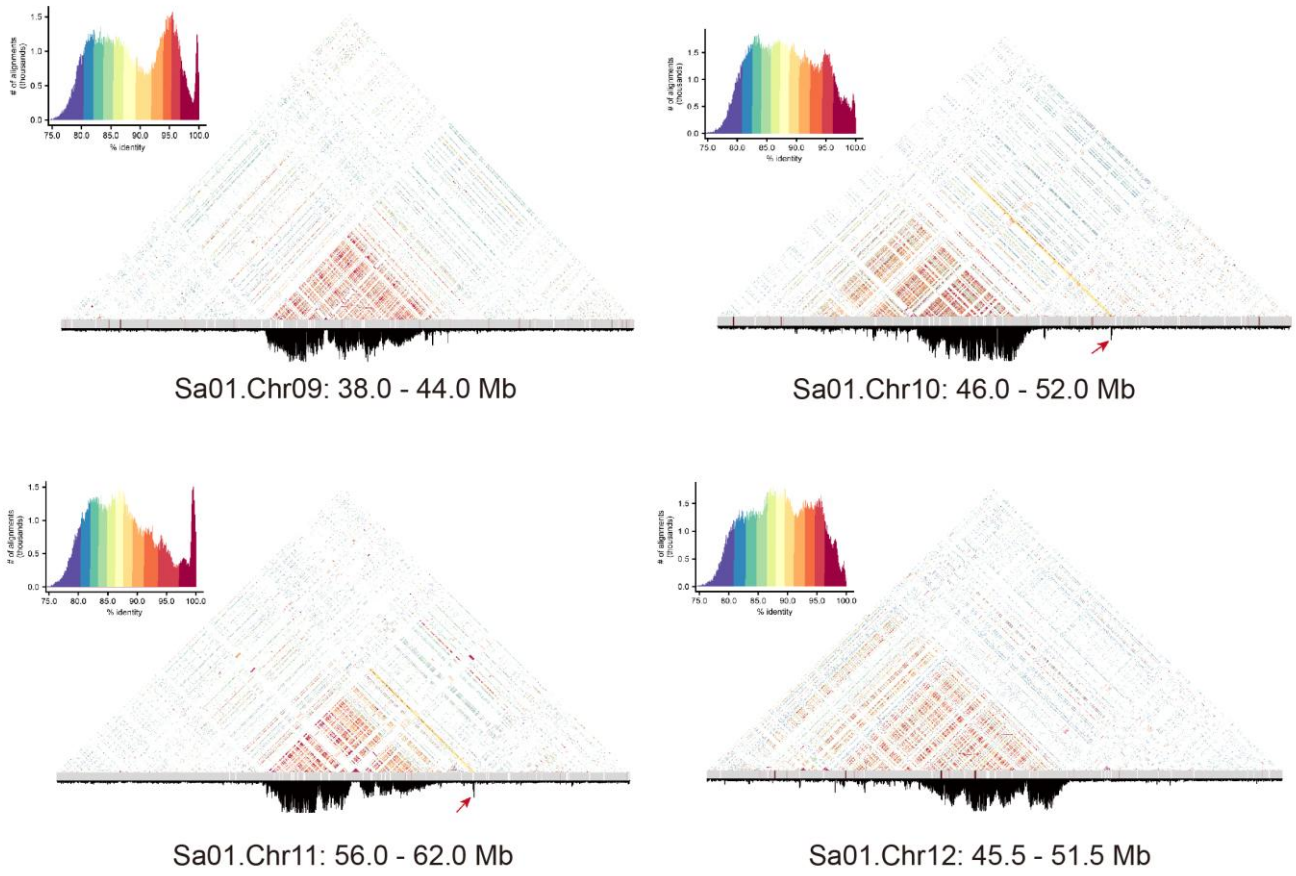

Fig. S21B. Pairwise sequence similarity around the functional centromeres of African eggplant. Heatmaps show the percentage sequence identity in pairwise 100-bp windows. Red arrows indicate potential artificial CENH3-binding peaks outside the functional centromeric regions. Chromosomes 9–12 are shown.

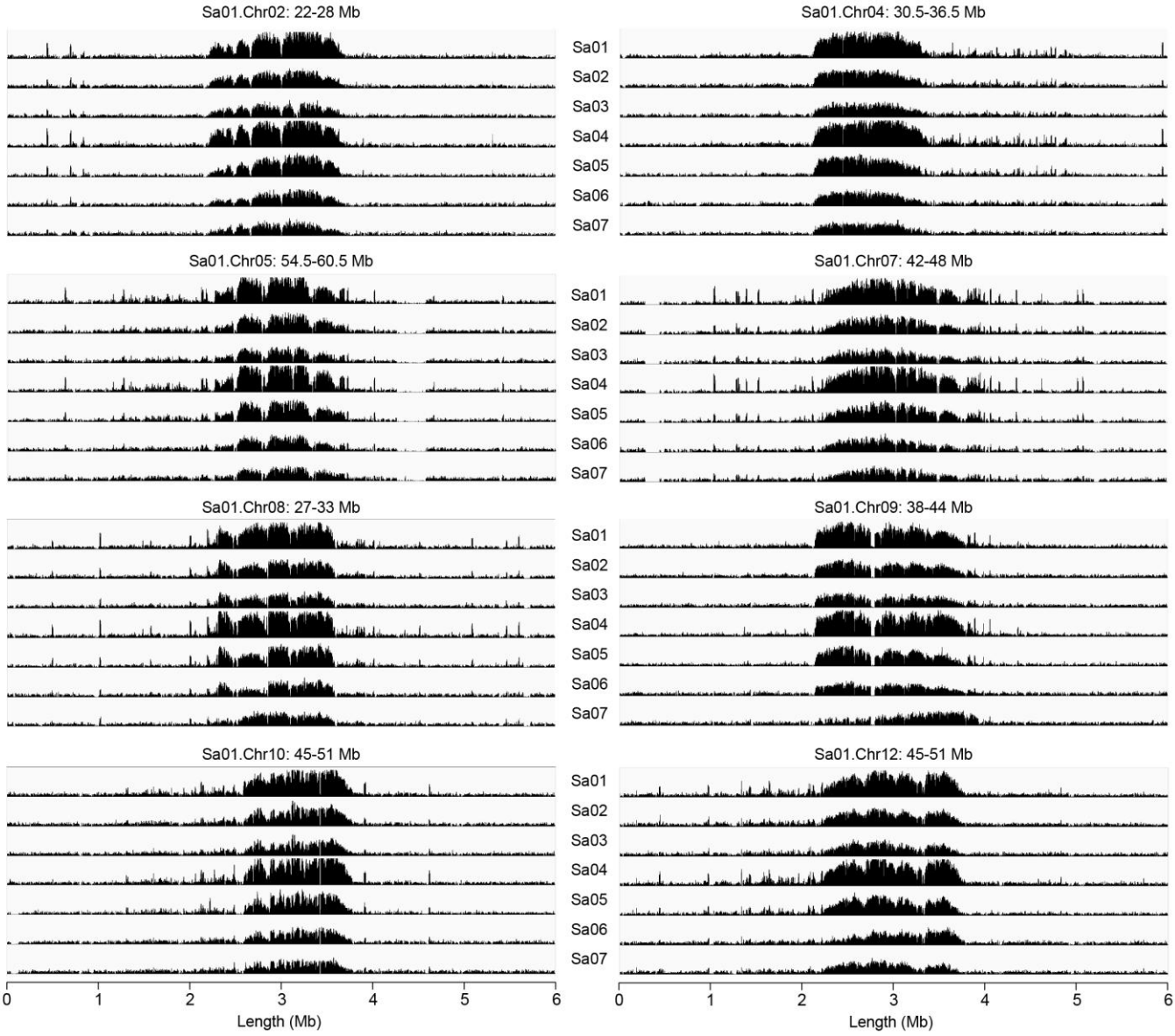

Fig. S22. Centromere diversity across seven African eggplant accessions. CENH3 ChIP-seq reads were mapped to the reference genome ‘Sa01’. Chromosomes without significant differences (Chr2, 4, 5, 7, 8, 9, 10, 12) are shown.